Removal of Chromium(VI) and Uranium(VI) from aqueous solution by the derivative of chitosan

2020

DU Xiaoyu

Doctoral program in Advanced Materials Science and Technology

Graduate School of Science and Technology

Niigata University

Contents

Chapter 1 General Introduction

1.1 Background

Toxic metal contamination in aquatic environments has attracted tremendous attention due to the rapidly increasing number of manufacturing industries. Heavy metals are of major environmental concern because they are non-biodegradable and cannot be decomposed or metabolized [1]. Heavy metals like lead chromium (Cr), uranium (U), mercury (Hg), zinc (Zn), and copper (Cu) gained the attention for their removal from wastewater because of their health hazards. Despite various regulations for heavy metals, industries which involve metal plating, painting, mining operations, battery manufacturing, are releasing lot of heavy metals in the water bodies [2].

It is well known that the major forms of environmental pollution include air pollution, water pollution, soil pollution and so on. Among them, water pollution is the most seriously due to its liquidity which may bring other pollution. Water is an indispensable resource for the survival of living organisms and natural ecosystems, covering about three-fourth of the Earth's surface [3]. However, more than 97 % of the net water supply is in the oceans and other saline water bodies, making it inapt for direct human consumption [4]. Furthermore, about 2.4 % of the remaining 3 % of water resources is trapped as soil/atmospheric moisture, glaciers, and ice caps, which are unreachable for daily usage. As a consequence, the main drinking water resources for humanity are the residual 0.6 % of fresh water resources in the form of rivers, lakes, and groundwater across the globe [5]. Heavy metals in environmental water have been a major preoccupation of their toxicity towards aquatic life, human beings and the environment [6].

There are several methods to remove metal ions in aqueous solutions. In these methods such as precipitation, adsorption and ion exchange, metal ions can interact with a solid surface [7]. However, these technologies become expensive or inefficient for the treatment of metal ions with high concentrations. Then, it is important to develop new methods for the removal and recovery of metals from such effluents, and thus reduce the concentration of these metal ions to low levels. Among environmentally friendly technologies for the removal of heavy metals from aquatic effluent, biosorption has attracted increasing research interest recently. The major advantages of biosorption are its high effectiveness in reducing the heavy metals and the use of inexpensive biosorbents. Biosorption studies using various low cost biomass as adsorbents have been currently performed widely for the removal of heavy metals from aquatic effluent. Biological adsorbent has the advantages of recyclable, low cost, easy operation and little possibility of secondary pollution [8, 9].

1.2 Heavy Metals

Heavy metals include lead (Pb), cadmium (Cd), zinc (Zn), mercury (Hg), arsenic (As), silver (Ag) chromium (Cr), uranium (U) iron (Fe), and the platinum group elements [10].

Heavy metals are of major environmental concern because they are non-biodegradable and cannot be decomposed or metabolized [11]. Several metals cause serious health and environment problems, and chromium (Cr) compounds are one of the most toxic contaminants in wastewater due to their high solubility and toxicity, and free transferability [12]. Cr has been widely applied in many industrial activities based on its excellent properties, for example, such as in electroplating, leather tanning, nuclear power plants, and textile industries [13,14]. Moreover, it can be used for anodizing, corrosion control, and chemical manufacturing [15-17].

Cr mainly exists in two oxidation states such as trivalent Chromium (Cr (III)) and hexavalent chromium (Cr (VI)) in natural aqueous environment. Hexavalent chromium (Cr (VI)) has been considered more hazardous to public health due to its mutagenic and carcinogenic properties [18]. Cr(VI) is high toxicity and carcinogen, environmental standard is less than 0.05 mg/L, drainage standard is less than 0.5 mg/L. At natural aqueous environment, it may be present form of CrO_4^{2-} or $HCrO_4^-$. On the hand, Cr(Ⅲ) is low toxicity, essential materials for living organisms, environmental standard is less than 2 mg/L. At natural aqueous environment, it tends to form $Cr(H_2O)_n(OH)_m(3\text{-}m)^+$ and Cr(Ⅲ)-organic complex.

It is well known that uranium (U) is one of the resources required to generate nuclear power and that it is ubiquitous in nature [19]. Although these features are advantages, it is very important to remember that U is a harmful pollutant in the natural environment. In particular, it has been pointed out that the mining and milling of U minerals generates a large amount of waste materials (tailings), which lead to environmental health damage [20-25]. To solve these problems, the proper management of U tailings by phytoremediation has been implemented recently [20,21]. This is because it is an environmentally friendly technology and uses plant biota to clean trace element contamination from soil [26]. To ensure ecosystem stability and public health, it is urgent to decrease the concentration of U(VI) to permissible limits in the environment [27].

From above-mentioned, Cr(VI) and U(VI) were selected for target elements in this work. The separation and reduction of Cr(VI) and U(VI) in wastewater is very important for environmental protection and human health.

1.3 Adsorbents

Different technologies for the removal of heavy metal ions are available such as chemical precipitation, coagulation, ion exchange, membrane technologies, adsorption. Adsorption has been proved as one of the most efficient methods for the removal of heavy metals from aqueous media [28]. The major advantages of biosorption are its high effectiveness, easy operation, no two pollution, and the use of inexpensive biosorbents.

1. 3. 1 Chitosan

Chitosan is a basic polysaccharide polymer with active functional groups, has unique physiological activity and physicochemical properties that can be used [29]. Chitosan is easily obtained due to the widespread natural occurrence of its source which is found in the shells of crustaceans, e.g., crabs, prawns, shrimps and insects. Further, chitin is easily converted to chitosan, the desired end product, through deacetylation [30]. Therefore, more and more pay attention to chitosan as a potential biosorbent for removal of heavy metal ions in water treatment since it has both amine and hydroxyl groups that can remove the heavy metal ions by forming stable metal chelates [31].

However, chitosan has some defects, such as notable swelling in aqueous media and nonporous structures, resulting in a very low surface area [32]. Therefore, many types of chemical modification can be undertaken to produce chitosan derivatives for improving the removal efficiency of the heavy metal [33]. For example, various chemical or physical modifications can be adopted for increasing the number of exposed active sites [34,35].

1. 3. 2 Cross-linked chitosan

It has been reported that chitosans have high potential for adsorption of chromium (Cr) [36-38]. Furthermore, cross-linked chitosan bead materials are fabricated by GA whose reaction is Schiff base between the aldehyde group of GA and the amide of chitosan. In this case, the amine groups and hydroxyl groups on the chitosan chain can act as chelation sites for Cr. Cross-linked chitosan bead materials with EP are mainly associated with hydroxyl groups due to EP. Thereby, the amino groups of chitosan are not damaged. Cross-linked chitosans are used to improve the adsorption behavior and to enhance the adsorption ability [39,40]. The adsorption capacity of cross-linked chitosan was investigated for the removal of heavy metal from aqueous solution under varying experimental conditions.

1. 3. 3 Sodium Dodecyl Sulfate (SDS) modified with chitosan

Among the many biosorbents available, chitosan can be an outstanding biosorbent for metals for the reason that its amine ($-NH_2$) and hydroxyl (-OH) groups may serve as coordination sites to form complexes with various heavy metal ions [41]. Chitosan has been proven to be very efficient as a biosorbent for the recovery of several toxic metals such as mercury (Hg), uranium (U), molybdenum (Mo), vanadium (V), and platinum (Pt) [42,43], and its full chemical name is called (1,4)-2-amino-2- deoxy-β-D-glucose. It can be employed as an environmentally friendly adsorbent due to it being economical and the fact that it does not result in secondary pollution. Chitosan can be produced by the alkaline deacetylation of chitin, which originates from the most abundant biopolymer-cellulose.

The uses of chitosan in the removal of various pollutants have been adequately reviewed [44]. In this work, we evaluated the adsorption of chitosan modified with sodium dodecyl sulfate (SDS) as part of the adsorption study of Cr using modified chitosan. The metal ion strength and the presence of key functional groups on the polymer chain allow its adsorption on surfaces [45-47]. The aggregation of particles through a bridging structure can be described as a two-step pathway: (1) initial chain adsorption and bridging, followed by (2) floc maturation/reconfiguration. Before the interparticle connection occurs, the chain of SDS must be adsorbed on a chitosan surface [48]. Furthermore, chitosan modified with SDS has recently been used for the removal of heavy metals, such as cadmium [49,50]. However, the use of SDS-modified chitosan as an adsorbent of Cr, with varying initial concentrations of SDS for optimizing the adsorbent, has rarely been evaluated. The objective of the present research was to investigate the efficiency of SDS-modified chitosan beads as a sorbent for Cr(VI) for more practical uses in the future, and to reveal the adsorption mechanism.

Moreover, the novel adsorbent can be recycled for adsorption heavy metal ions compared with the disposable adsorbent.

1.4 Theory

1. 4. 1 Adsorption capacity and Partition coefficient (PC) [51-54]

Many studies have shown that, the adsorption performance is usually evaluated and expressed by the maximum (or equilibrium) adsorption capacity. For data analysis, various equilibrium, kinetic, and thermodynamic models (equations) were employed to interpret the data and establish the extent of adsorption. The metallic ions uptake by each adsorbent was calculated using the Eq. (1):

$$q_e = \frac{(C_i - C_e)}{m} \cdot V \qquad (1\text{-}1)$$

where qe represents the adsorption capacities at equilibrium ($mg \cdot g^{-1}$), C_i and C_e are the initial and equilibrium concentrations of Cr in a batch system, respectively (mg·L-1); V is the volume of the solution (L); and m is the weight of adsorbent (g)

However, the maximum adsorption capacity is sensitively affected by the initial concentration of target pollutant (or more specifically, what is left after the sorption reaction). When the sorbent is exposure to a higher concentration of goal targets, it is likely to exhibit a higher adsorption capacity. On the other hand, when the sorbent is exposed to lower levels of target species, it will show lower capacities. Therefore, in addition to the maximum adsorption capacity, it is effective to estimate using the concept of the partition coefficient (PC).

PC = adsorption capacity / final concentration (1-2)

1. 4. 2 Langmuir and Freundlich Isotherm Models [55-57]

Langmuir and Freundlich isotherms were modeled in order to evaluate the performance of adsorbents in adsorption processes by the relationship between the

metal uptake (q_e) and the concentration of heavy metal ion (C_e) at equilibrium. Langmuir and Freundlich adsorption isotherms can be expressed, respectively.

The Langmuir isotherm equation is defined as follows:

$$\frac{C_e}{q_e} = \frac{C_e}{q_{\max}} + \frac{1}{K_L q_{\max}} \qquad (1\text{-}3)$$

where C_e is the concentration of *heavy metal ion* at equilibrium ($mg \cdot dm^{-3}$), q_e and q_{max} are the amount of adsorption of *heavy metal ion* at equilibrium ($mg \cdot g^{-1}$) and the maximum adsorption capacity by the adsorbents ($mg \cdot g^{-1}$) respectively, K_L ($dm^{-3} \cdot mg^{-1}$) is the adsorption constant of Langmuir isotherm.

The linearized Freundlich isotherm equation is defined as follows:

$$\log_{10} q_e = \log_{10} K_F + (1/n) \log_{10} C_e \qquad (1\text{-}4)$$

In this equation, K_F is the adsorption capacity ($(mg \cdot g^{-1}) \cdot (dm^{-3} \cdot mg^{-1})^{1/n}$), *1/n* is the adsorption intensity. The values of *1/n* and K_F were determined on the basis of the plots of q_e versus C_e in log scale.

1. 4. 3 Kinetic Models [58-60]

Kinetic models have been proposed to determine the rate of adsorption of the adsorbent. In addition, the process of kinetic study is very important for understanding the reaction process and the rate of adsorption reactions.

The pseudo first-order model is given by the following equation:

$$\ln(q_e - q_t) = \ln(q_e) - k_1 t \qquad (1\text{-}5)$$

where q_e and q_t are the adsorption capacity of heavy metal ion using the adsorbents at equilibrium and time *t*, respectively ($mg \cdot g^{-1}$), and k_1 is the rate constant of the pseudo-

first-order adsorption (h^{-1}).

The pseudo-second order rate equation is expressed as follows:

$$\frac{t}{q_t} = \frac{1}{kq_e^2} + \frac{t}{q_e} \qquad (1\text{-}6)$$

where k ($g \cdot mg^{-1} \cdot h^{-1}$) is the rate constant of the second-order model, and q_e and q_t are the adsorption capacities of heavy metal ion using the adsorbents at equilibrium and time t, respectively ($mg \cdot g^{-1}$).

The adsorption capacity of adsorbents for heavy metal ion was calculated using the mass balance equation:

$$q_e = \frac{(C_i - C_e)}{m} \cdot V \qquad (1\text{-}7)$$

where q_e is the adsorption capacity ($mg \cdot g^{-1}$) of heavy metal ion by the adsorbents at equilibrium, C_i and C_e are the concentrations of heavy metal ion at initial and equilibrium in a batch system respectively ($mg \cdot dm^{-3}$), V (dm^{-3}) is the volume of the heavy metal solution, and m (g) is the mass of the adsorbents.

1. 4. 4 Thermodynamics Studies [61,62]

Thermodynamic considerations of an adsorption process are necessary to conclude whether the process is spontaneous or not. The Gibb's free energy change, ΔG, is an indication of spontaneity of a chemical reaction and therefore is an important criterion for spontaneity. Both standard enthalpy (ΔH) and standard entropy (ΔS) can be considered to determine the Gibb's free energy of the process. The free energy of an adsorption process is related to the equilibrium constant by the Van't Hoff equation :

$$\Delta G^0 = -RT \ln K_d \qquad (1\text{-}8)$$

where R is the universal gas constant (8.314Jmol^{-1}·K^{-1}), T is the temperature (K), Value of ln K_d can be obtained by plotting ln (q_e/C_e) vs. q_e for adsorption of metallic ions onto adsorbrnts and extrapolating q_e to zero. The thermodynamic parameters of the adsorption for the equations were also calculated by using the Langmuir constant (K_L) or Freundlich constants (K_F) instead of K_d.

$$\ln K_d = \frac{\Delta S^0}{R} - \frac{\Delta H^0}{RT} \qquad (1\text{-}9)$$

The slope and intercept of the Van't-Hoff plot of ln$k$ vs. 1/T were used to determine the values of ΔH and ΔS based on eq. 14. The plot of ΔG vs.T also can give the ΔH and ΔS by the following equation.

$$\Delta G^0 = \Delta H^0 - T\Delta S^0 \qquad (1\text{-}10)$$

1.5 Instrumental Analysis

After the synthesis, the prepared adsorbent was characterized by different techniques such as scanning electron microscopy-energy dispersive X-ray spectroscopy (SEM-EDS), X-ray photoelectron spectroscopy (XPS) and Fourier transform-infrared spectroscopy (FT-IR). We used inductively coupled plasma mass spectrometry (ICP-MS) for the determination of Cr(VI) and U(VI) in solution.

1. 5. 1 SEM-EDS [63,64]

Scanning electron microscopy (SEM) is a method for high-resolution imaging of surfaces. The SEM uses electrons for imaging, much as a light microscope uses visible light. The advantages of SEM over light microscopy include much higher magnification (>100,000X) and greater depth of field up to 100 times that of light microscopy. Qualitative and quantitative chemical analysis information is also obtained using an energy dispersive x-ray spectrometer (EDS) with the SEM.

Energy Dispersive X-Ray Spectroscopy (EDS) is a chemical microanalysis technique used in conjunction with scanning electron microscopy (SEM). The EDS technique detects x-rays emitted from the sample during bombardment by an electron beam to characterize the elemental composition of the analyzed volume. Features or phases as small as 1 μm or less can be analyzed. When the sample is bombarded by the SEM's electron beam, electrons are ejected from the atoms comprising the sample's surface. The resulting electron vacancies are filled by electrons from a higher state, and an x-ray is emitted to balance the energy difference between the two electrons' states. The x-ray energy is characteristic of the element from which it was emitted.

1. 5. 2 X-Ray Photoelectron Spectroscopy (XPS) [65,66]

X-Ray Photoelectron Spectroscopy (XPS), also known as Electron Spectroscopy for Chemical Analysis (ESCA), is an analysis technique used to obtain chemical information about the surfaces of solid materials. Both composition and the chemical state of surface constituents can be determined by XPS. Insulators and conductors can easily be analyzed in surface areas from a few microns to a few millimeters across.

The sample is placed in an ultrahigh vacuum environment and exposed to a low-energy, monochromatic x-ray source. The incident x-rays cause the ejection of core-level electrons from sample atoms. The energy of a photoemitted core electron is a function of its binding energy and is characteristic of the element from which it was emitted. Energy analysis of the emitted photoelectrons is the primary data used for XPS. When the core electron is ejected by the incident x-ray, an outer electron fills the core hole. The energy of this transition is balanced by the emission of an Auger electron or a characteristic x-ray. Analysis of Auger electrons can be used in XPS, in addition to emitted photoelectrons.

The photoelectrons and Auger electrons emitted from the sample are detected by an electron energy analyzer, and their energy is determined as a function of their velocity entering the detector. By counting the number of photoelectrons and Auger electrons as a function of their energy, a spectrum representing the surface composition is obtained. The energy corresponding to each peak is characteristic of an element present in the sampled volume. The area under a peak in the spectrum is a measure of

the relative amount of the element represented by that peak. The peak shape and precise position indicates the chemical state for the element.

1. 5. 3 Fourier Transform-Infrared Spectroscopy (FTIR) [67-69]

Fourier Transform-Infrared Spectroscopy (FTIR) is an analytical technique used to identify organic (and in some cases inorganic) materials. This technique measures the absorption of infrared radiation by the sample material versus wavelength. The infrared absorption bands identify molecular components and structures.

When a material is irradiated with infrared radiation, absorbed IR radiation usually excites molecules into a higher vibrational state. The wavelength of light absorbed by a particular molecule is a function of the energy difference between the at-rest and excited vibrational states. The wavelengths that are absorbed by the sample are characteristic of its molecular structure.

The FTIR spectrometer uses an interferometer to modulate the wavelength from a broadband infrared source. A detector measures the intensity of transmitted or reflected light as a function of its wavelength. The signal obtained from the detector is an interferogram, which must be analyzed with a computer using Fourier transforms to obtain a single-beam infrared spectrum. The FTIR spectra are usually presented as plots of intensity versus wavenumber (in cm-1). Wavenumber is the reciprocal of the wavelength. The intensity can be plotted as the percentage of light transmittance or absorbance at each wavenumber.

1. 5. 4 Brunauer-Emmett-Teller (BET) surface area analysis [70,71]

The determination of specific surface areas represents a major task regarding the characterization of porous and finely-dispersed solids. Gas adsorption is the appropriate method to solve this task. If a gas gets in contact with a solid material a part of the dosed gas molecules is being adsorbed onto the surface of this material. The adsorbed amount of gas depends on the gas pressure, the temperature, the kind of gas and the size of the surface area. By means of the BET equation the amount of adsorbed gas, which build up one monolayer on the surface, can be calculated from the measured isotherm. The amount of molecules in this monolayer multiplied by the required space of one molecule gives the BET surface area. After choosing the measuring gas and temperature, the specific surface area of a solid material can be reliably and comparably calculated from the adsorption isotherm. Due to practical reasons the adsorption of Nitrogen at a temperature of 77 K (liquid Nitrogen) has been established as the method for the determination of specific surface areas.

1. 5. 5 Inductively coupled plasma mass spectrometry (ICP-MS) [72-74]

Inductively coupled plasma mass spectrometry (ICP-MS) is a type of mass spectrometry that uses an Inductively coupled plasma to ionize the sample. It atomizes the sample and creates atomic and small polyatomic ions, which are then detected. It is known and used for its ability to detect metals and several non-metals in liquid samples at very low concentrations. It can detect different isotopes of the same element, which makes it a versatile tool in Isotopic labeling. Compared to atomic absorption spectroscopy, ICP-MS has greater speed, precision, and sensitivity.

1. 6 Outline of the Thesis

The environmental conservation is of increasing social and economic importance. One of the intractable environmental problems is water pollution by heavy metals. Heavy metals in environmental water have been a major preoccupation for many years because of their toxicity towards aquatic life, human beings and the environment.

Due to serious hazardous effects of heavy metal ions on human health and toxicity in the environment, it is important to develop a simple and highly effective removal method as well as sensitive analytical method for environmental pollutants to improve the quality of environment and human life.

In this thesis, the objective heavy elements are chromium (Cr) and uranium (U). The purpose of present study is to develop the elimination method of Cr and U by cross-linked chitosan and Cr by SDS-chitosan, to investigate the efficiency of these chitosan derivative as an adsorbent for heavy metals for more practical uses in the future, and to reveal the adsorption mechanism.

In this paper, there are 5 chapters.

In Chapter 1, the general introduction was stated.

In Chapter 2, the adsorption of Cr(VI) onto chitosan modified with EP and GA was performed. This study investigated the adsorption of Cr(VI) by cross-linked chitosan. Adsorption experiments from aqueous solutions containing known amounts of Cr(VI) was explored in a batch system. The amount of Cr(VI) adsorbed at different pH values, initial concentrations, sorbent dosages, contact times, and temperature were determined by ICP-MS in order to determine the optimum conditions for Cr(VI)

adsorption. The metals adsorption on cross-linked chitosan conformed to the Langmuir isothermal adsorption equation. Overall the modified chitosan exhibited a higher adsorption capacity and stronger chemical affinity than pristine chitosan. The rates of adsorption were found to conform to pseudo-second order kinetics. Furthermore, to evaluate the characteristics of the sample used in this work, the surface morphology of the chitosan (both modified and pristine chitosan) was determined by N_2-BET, SEM and FT-IR.

In Chapter 3, the adsorption of U(VI) onto chitosan modified with EP and GA was performed. The modifying chitosan cross-linked was used as an adsorbent for the removal of U(VI) from aqueous solutions. The adsorption potential of U(VI) by the materials was investigated by varying experimental conditions such as pH, contact time and the dosage of the modifying chitosan cross-linked. Adsorption isotherms of U(VI) onto the cross-linked chitosan were studied with varying initial concentrations under optimum experiment conditions. The surface properties of the modified chitosan were characterized by SEM and FT-IR. Furthermore, the adsorption mechanism of U(VI) by each material was investigated by applying Langmuir and Freundlich isotherm equations to the data obtained. In case of U(VI), the modified chitosan also exhibited a higher adsorption capacity and stronger chemical affinity than pristine chitosan.

In Chapter 4, the adsorption of Cr(VI) by chitosan beads modified with sodium dodecyl sulfate (SDS) was conducted. In this study, chitosan beads modified SDS were successfully synthesized and employed for the removal of Cr(VI). The adsorption performance of the adsorbent (SDS-chitosan beads) was examined by batch

experiments. The partition coefficient (PC) as well as the adsorption capacity were evaluated to assess the true performance of the adsorbent in this work. The adsorbent (SDS-chitosan beads) showed a maximum Cr(VI) adsorption capacity of 3.23 $mg \cdot g^{-1}$ and PC of 9.5 $mg \cdot g^{-1} \cdot mM^{-1}$ for Cr(VI). The prepared adsorbent was characterized by different techniques such as scanning electron microscopy-energy dispersive (SEM-EDS), X-ray photoelectron spectroscopy (XPS) and Fourier transform infrared spectroscopy (FT-IR). We used inductively coupled plasma mass spectrometry (ICP-MS) for the determination of Cr(VI) in solution. The experimental data could be well-fitted by pseudo-second-order kinetic and Langmuir isotherm models. The thermodynamic studies indicated that the adsorption process was favourable under the higher temperature condition. The SDS-modified chitosan beads synthesized in this work represent a promising adsorbent for removing Cr(VI).

In Chapter 5, the conclusions of the thesis are presented.

Chapter 2 Removal of Chromium from Aqueous Solution Using Cross-linked Chitosan

2. 1 Introduction

As is well known, the investigations on abundant levels of toxic heavy metal ions (e.g., hexavalent chromium, Cr(VI)) discharged to the environment (and its persistence in the environment) have now being received considerable attention with the development of society and the industrial economy [75,76]. Several metals caused serious health and the environment problems, chromium(Cr) compounds are one of the most toxic contaminants in wastewater due to their high solubility and toxicity, and free transferability [77,78]. The water that we drink may contain industrial wastewater with chromium [79].

Cr mainly consists of two stable oxidation states such as trivalent state Cr(III) and hexavalent state Cr(VI) in natural aqueous environment. Cr(VI) may be present in the form of CrO_4^{2-} or $HCrO_4^-$, whereas Cr(III) tends to form $[Cr(H_2O)_6]^{3+}$, $Cr(H_2O)_5(OH)^{2+}$, $Cr(H_2O)_4(OH)_2^+$, or Cr(III) organic complexes. It is well known that Cr(III) is essential materials for living organisms, whereas Cr(VI) is more toxic, carcinogenic, and mutagenic [80,81].

Therefore the separation and reduction of chromium in waste water is very important for environmental protection and human health. Various treatment technologies such as ion exchange, precipitation, ultrafiltration, reverse osmosis and electro dialysis have been used for the removal of heavy metal ions from aqueous solution. However, these processes have some disadvantages, such as high consumption of reagent and energy, low selectivity, high operational cost, and difficult further treatment due to generation of toxic sludge [82].

The aim of this paper is to investigate the adsorption efficiency of cross-linked for more practical use in the future. Adsorption isotherms of Cr(VI) and U(VI) was studied and analyzed using Langmuir and Freundlich equations, and kinetics analyses were also carried out. In addition, to evaluate the characteristics of the sample used in this work, the surface morphology of the carbon was determined by SEM (scanning electron microscope) and FT-IR (Fourier transform infrared spectroscopy).

2. 2 Experimental Sections

2. 2. 1 Materials and Reagents

Chitosan was prepared from purified natural shells of crustacean contained chitin about 30%. Chitosan was stirred with the acetic acid solution 200 ml (2.0%) and added drop-wise to 100mL of 0.5M NaOH.

Chitosan was added to 1.0wt% of EP, adjust the pH to 14. After keeping the mixed solution at 60 ℃ for 6h, we can get cross-linking with EP. Chitosan was added to 1.0wt% of GA, adjust the pH to 7. After keeping the mixed solution at room temperature for 24h, we can get cross-linking with GA.

Cr(VI) standard solutions were prepared by diluting a standard solution (1,000 $mg \cdot dm^{-3}$ $K_2Cr_2O_7$ solution), which was both purchased from Kanto Chemical Co. Inc. All other chemical reagents were also purchased from Kanto Chemical Co., Inc. All reagents used were of analytical grade, and water (>18.2 MΩ in electrical resistance) which was treated by an ultrapure water system (Advantec aquarius: RFU 424TA, Advantec Toyo, Japan) was employed throughout the work.

2. 2. 2 Experiment of Apparatus

The morphology of cross-linked chitosan was characterized by a SEM (JSM-5800, JEOL, Ltd.). The material was placed on a microgrid of silicon, and transferred to the analysis chamber in the SEM equipment.

The cross-linked chitosan was also investigated using FTIR spectroscopy (FTIR-4200, Jasco, Corporation) to identify the functional groups. For FTIR in pressed KBr pellets, the sample was washed three times with ethanol for 5 min, filtered, and dried at

110 °C for 24 h. The spectral resolution was set to 1 cm^{-1}, and 150 scans were collected for each spectrum.

The specific surface areas and pore volumes of cross-linked chitosan were measured by N_2 adsorption/desorption using a surface area and pore size analyzer (TriStar II 3020, Micromeritics, Instrument Corporation) after vacuum degassing of the sample in the tube at 200 °C for 12 h.

An ICP-MS (Inductively Coupled Plasma Mass Spectrometry) instrument (Thermo Fisher Scientific X_2) was used to determine the concentration of Cr(VI). Replicate experiments were basically performed three times. The operating conditions of ICP-MS are shown in Table 2-1.

2. 2. 3 Sorption Experiment of Cr(VI) Using Cross-linked Chitosan

The adsorption capacities of Cr from aqueous solution of the cross-linked chitosan were investigated by a batch method. Cross-linked chitosan was thoroughly mixed with 100 cm^3 of containing known amount of Cr (VI) in a 200 cm^3 conical flask, and the suspensions was shaken by an automatic shaker (PLUS SHAKER EP-1, TAITEC, Corporation) in a water bath at room temperature (25 ± 2 °C). Sorption experiments were conducted by varying the pH (1-7), contact time (0.5h-24h), sorbent dosage (0.1-0.5 $g \cdot dm^{-3}$). The pH of each solution was adjusted by using 0.1 $mol \cdot dm^{-3}$ NaOH and 0.1 $mol \cdot dm^{-3}$ HNO_3.

Adsorption isotherms of Cr (VI) onto cross-linked chitosan was measured at varying initial Cr concentrations (0.05-5.0 $mg \cdot dm^{-3}$) under optimized conditions.

Following each sorption experiment, the suspension containing cross-linked

chitosan and the above standard solution was filtered through a 0.45 μm membrane filter (Advantec Mixed Cellulose Ester, 47 mm) to remove Cr(VI) that have been adsorbed into the cross-linked chitosan. Then the concentration of this metal in the filtrate was determined with an ICP-MS.

2. 3 Results and Discussion

2. 3. 1 Characteristics of Cross-linked Chitosan

The morphologies of pristine and cross-linked chitosan characterized by SEM are shown in Fig. 2-1. Moreover, the surface properties including specific surface areas of pristine and modified chitosan determined by N_2-BET method are shown in Table 2-2. Judging from the SEM images of the chitosan and the cross-linked chitosan in Fig. 2-2, it can be observed that surface texture were changed. This is consistent with the data of the specific surface area in Table 2-2. The specific surface area of modified chitosan were remarkably increased.

The FTIR spectra of pristine and modified chitosan are shown in Fig. 2-2. The broad and intense peak at 3400 to 3500 cm^{-1} corresponds to the O-H and -NH_2 stretching vibration of hydroxyl groups of chitosan and the cross-linked chitosan. [83-85]. The peak at 2871 cm^{-1} is related to aliphatic methylene group. But the wide peak at 1560 to 1640 cm^{-1} shows the mine group of remarkable for GA [84].

Then, we examined the adsorption of Cr(VI) on pristine and modified chitosan have been carried out at the present work.

2. 3. 2 Effect of pH

Solution pH is one of the most important parameters affecting adsorption characteristics. In order to investigate the effects of solution pH on the uptake of Cr(VI), sorption experiments were conducted at different pH values at room temperature 25 °C, while the concentration of Cr(VI) was kept constant at 500 ppb, and adsorbent dosage was 0.1g·dm^{-3}. The contact time was 6 h.

The results for Cr(VI) are shown in Fig 2-3, it can be seen that the uptake of Cr(VI) is effective even at pH 1-3 by cross-linking and that the adsorption capacity of Cr(VI) reaches maximum at pH 4 for the adsorbents, which is due to the changes of the surface charge of the adsorbent. The reason is as follows. At lower pH, the surface of the adsorbent may become protonated and more positively charged which would attract the chromate anions more. At higher pH, the hydroxyl ions in the solution may be combined with chromate ions to form precipitates. Aqueous solution pH can affect the surface charge of the adsorbent, the degree of ionization, speciation of metal ions, and surface metal binding sites.

On the other hand, Fig 2-4 shows the pH dependence of hydrogen chromate anion distribution. It can be seen that Cr(VI) exists as neutral chromic acid (H_2CrO_4) between pH 1.0 and pH 2.0, as hydrogen chromate anion ($HCrO4^-$) between pH 2.0 and pH 6.5, and as chromate anion (CrO_4^{2-}) above pH 6.5. There are several forms of Cr(VI) ion existing in solution, i.e., chromate (CrO_4^{2-}), dichromate ($Cr_2O_7^{2-}$) and hydrogen chromate ($HCrO_4^-$). These ionic forms are related to the solution pH and total chromate concentration [85]. The uptake of Cr(VI) deceased with the increase of pH, on the one hand, because of the higher concentration of OH^- ions present in the mixture that competes with Cr(VI) species [86]. On the other hand, NH_2 groups were deprotonated and formed negatively charged sites with pH increasing, producing electrostatic repulsion between negatively charged sites and negatively charged hexavalent chromium ions that decrease the amount of Cr(VI) adsorption [87].

2. 3. 3 Effect of Contact Time

The effect of contact time on the adsorption capacity of Cr(VI) using 0.2 $g \cdot dm^{-3}$ adsorbents (500 $\mu g \cdot dm^{-3}$ of Cr solution) is investigated at pH 4 at room temperature 25 °C.

The adsorption capacity of adsorbents for Cr(VI) increased sharply within the first 9 h, which may be attributable to the availability of the sites on the surface of the adsorbent. It is suggested that a concentration gradient is present in both the adsorbent and adsorbate in the solution [85]. Then, it reached adsorption equilibrium at 12 h, and afterwards, there was no appreciable increase (Fig 2-6). Hence, the optimized contact time was taken to be 12 h for further studies.

2. 3. 4 Adsorption Isotherms

Adsorption isotherms are commonly used to reflect the performance of adsorbents in adsorption processes. In this paper, Langmuir and Freundlich isotherms were applied to the data obtained in this work. The linear plots of C_e and m were presented for Langmuir and Freundlich models (Fig 2-5), and the coefficient of both isotherms are shown in Table 2-3 and 2-4. From Fig 2-5, it is also found that chitosan is more fitted to Langmuir isotherm, EP and GA compared to Chitosan, fitted to Frendlich as well as Langmuir. Adsorption isotherms of Cr(VI) on the modified chitosan can be generally described by Langmuir isotherm more satisfactorily. The adsorption may have occurred mainly by monolayer reaction.

From Table 2-3 and 2-4, the maximum adsorption capacity of modified chitosan reached 90.9 mg/g from 49.8mg/g by cross-linked with EP under our experimental

conditions. That is to say, modified chitosan by cross-linking can be an efficient adsorbent for Cr(VI).

2. 3. 5 Kinetic Studies

When we added the adsorbents 0.20g/L, Cr(VI) 500μg/L, adjusted pH was 4. From Fig 2-4, 2-5, 2-6 and Table 2-5, Table 2-6, 2-7 the rates of adsorption by chitosan were found to more conform to pseudo-second order kinetics. The rates of adsorption using the modified chitosan for the removal of Cr were found to conform to pseudo-second order kinetics.

2. 3. 6 Thermodynamic Studies

The Thermodynamic parameters for the adsorption of Cr(VI) onto adsorbent was shown in Table 2-8, Table 2-9 and Table 2-10. A plot of $\ln K_d$ versus $1/T$ was shown in Fig 2-7. The negative value of ΔG indicated the adsorption process is highly favorable and spontaneous, and it is more negative at higher temperature, which indicates that the adsorption process increases with the rise in temperature. The value of ΔH indicates that the adsorption force perhaps is hydrogen-bonding force. The positive value of entropy change (ΔS) implies some structural changes in adsorbate and adsorbent during the adsorption process, which reflects the affinity of the adsorbent towards the adsorbate species. In addition, positive value of ΔS suggests increased randomness at the solid/solution interface with some structural changes in the adsorbate and the adsorbent.

The adsorbed ions, which are displaced by the adsorbate species, gain more translational entropy than is lost by the adsorbate ions, thus allowing for the prevalence of randomness in the system.

2. 3. 7 Mechanism of Cr(VI) sorption on cross-linking chitosan.

Chitosan can be an excellent biosorbent for metals because its amine ($-NH_2$) and hydroxyl (-OH) groups may serve as coordination sites to form complexes with various heavy metal ions. In order to increase the number of exposed active sites, regard to chitosan cross-linked EP, amino groups of chitosan were not damaged during the process of cross-linking because EP are mainly associated with hydroxyl groups. In the case of chitosan cross-linked GA, the reaction of Schiff base between the aldehyde group of GA and the amido of chitosan is dominant. The mechanism of Cr(VI) sorption on cross-linking chitosan as shown in the Fig 2-8.

2. 4 Conclusions

The efficiency of cross-linked chitosan as an adsorbent for Cr(VI) was investigated. From this work, the following matters were clarified:

(1) The uptake of Cr(VI) was performed even at pH 1-3 by cross-linking. The adsorption capacity of Cr(VI) reached maximum at pH 4 for the adsorbents.

(2) The maximum adsorption capacity of modified chitosan reached 90.9mg/g from 49.8mg/g by cross-linking with EP under our experimental conditions.

(3) Adsorption isotherms of Cr on the modified chitosan can be generally described by Langmuir isotherm more satisfactorily. The adsorption may have occurred mainly by monolayer reaction.

(4) The rates of adsorption using the modified chitosan for the removal of Cr were found to conform to pseudo-second order kinetics.

(5) The negative value of ΔG indicated the adsorption process is highly favorable and spontaneous, and it is more negative at higher temperature, which indicates that the adsorption process increases with the rise in temperature. The value of ΔH indicates that the adsorption force perhaps is hydrogen-bonding force. The positive value of entropy change (ΔS) implies some structural changes in adsorbate and adsorbent during the adsorption process, which reflects the affinity of the adsorbent towards the adsorbate species. In addition, positive value of ΔS suggests increased randomness at the solid/solution interface with some structural changes in the adsorbate and the adsorbent.

From these results, to treatment the industrial wastewater of 500 L/Hr that need

cross-linked chitosan with EP is 3.3g. Compare to carbon used 548g, it was quantitatively clarified to some extent that cross-linked chitosan can be an efficient sorbent for Cr(VI), which provide very significant information from the viewpoint of environmental protection.

Tables

Table 2-1 Operating conditions of inductively coupled plasma mass spectrometry (ICP-MS).

RF power	1400 W
Plasma gas flow	15 l·min^{-1}
Carrier gas flow	1.2 l·min^{-1}
Sampling depth	6.5 mm
Sample uptake rate	0.5 ml·min^{-1}
Measurement point	3 points/peak
Integration time	1.0 sec/point
Measured isotope	^{52}Cr

Table 2-2 Surface properties of the pristine chitosan and cross-linked chitosan.

Adsorbent	Chitosan	EP	GA
BET surface area (m^2/g)	0.80	8.26	52.1

Table 2-3 Coefficient of Langmuir isotherms for Cr(VI)

	Chitosan	EP	GA
a (mg/g)	49.8	90.9	73.5
b (L/mg)	2.87	0.558	0.594
R_L	0.0337	0.152	0.144
R^2	0.979	0.989	0.997

Table 2-4 Coefficient of Frendlich isotherms for Cr(VI)

K_F	26.4	36.2	30.8
1/n	0.841	0.721	0.685
R^2	0.941	0.980	0.977

Table 2-5 Pseudo-first or second-order model kinetic parameters of Cr(VI) on chitosan

	Pseudo-first-order model	Pseudo-second-order model	
$K_1(h^{-1})$	0.330	K_2(g/mg h)	0.135
$q_e(mg/g)_{exp}$	2.23	$q_e(mg/g)_{exp}$	2.23
q_e $(mg/g)_{cal}$	1.66	q_e $(mg/g)_{cal}$	2.26
R^2	0.980	R^2	0.983

Table 2-6 Pseudo-first-order model kinetic parameters of Cr(VI)

	Chitosan	EP	GA
K_2(g/mg h)	0.135	0.226	0.0975
$q_e(mg/g)_{exp}$	2.23	2.21	2.29
q_e $(mg/g)_{cal}$	2.26	2.44	2.72
R^2	0.983	0.989	0.935

Table 2-7 Pseudo- second-order model kinetic parameters of Cr(VI)

	Chitosan	EP	GA
K_2(g/mg h)	0.135	0.226	0.0975
$q_e(mg/g)_{exp}$	2.23	2.21	2.29
q_e $(mg/g)_{cal}$	2.26	2.44	2.72
R^2	0.983	0.989	0.935

Table 2-8 Thermodynamic parameters for Chitosan

T(K)	ΔH(kJ/mol)	ΔS(J/mol・K)	ΔG(kJ/mol)
288	22.9	85.9	-1.890
298	-	-	-2.749
308	-	-	-3.608
318	-	-	-4.467

Table 2-9 Thermodynamic parameters for EP

T(K)	Δ*H*(kJ/mol)	Δ*S*(J/mol・K)	Δ*G*(kJ/mol)
288	8.38	39.4	-2.96
298	-	-	-3.35
308	-	-	-3.74
318	-	-	-4.14

Table 2-10 Thermodynamic parameters for EP

T(K)	Δ*H*(kJ/mol)	Δ*S*(J/mol・K)	Δ*G*(kJ/mol)
288	28.3	117.8	-5.68
298	-	-	-6.86
308	-	-	-8.04
318	-	-	-9.21

Figures

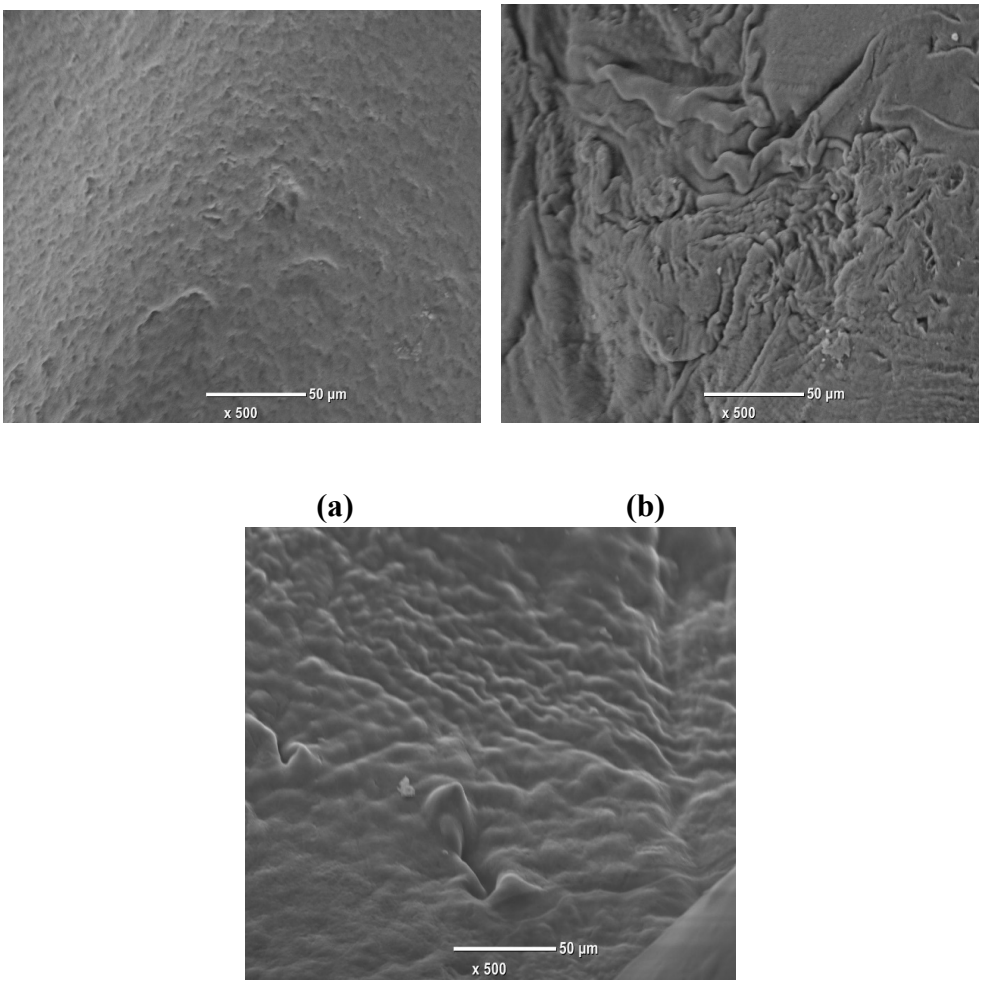

Fig. 2-1 The SEM images of pristine and modified chitosan (a) pristine; (b) crosslinked with EP; (c) crosslinked with GA.

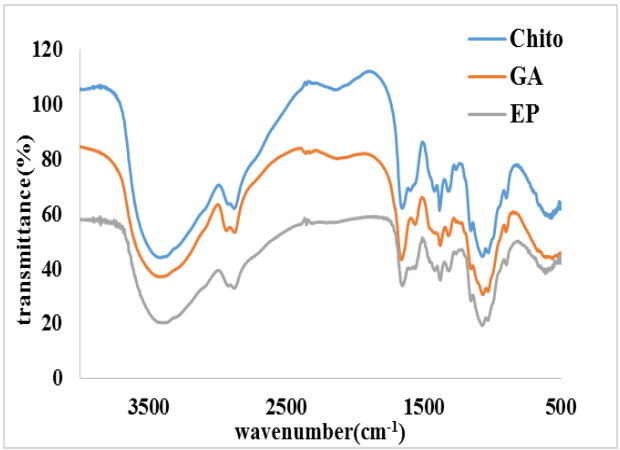

Fig. 2-2 The FTIR spectra of pristine and modified chitosan.

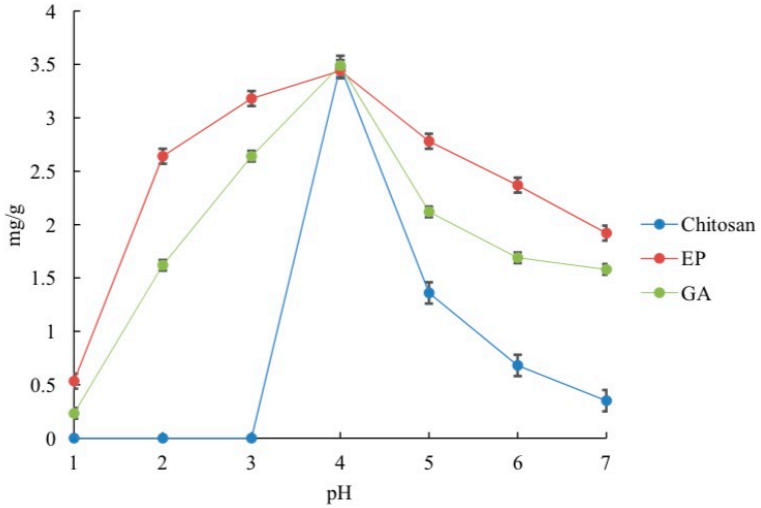

Fig. 2-3 Effect of pH on percent removal of Cr using chitosan, EP and GA.

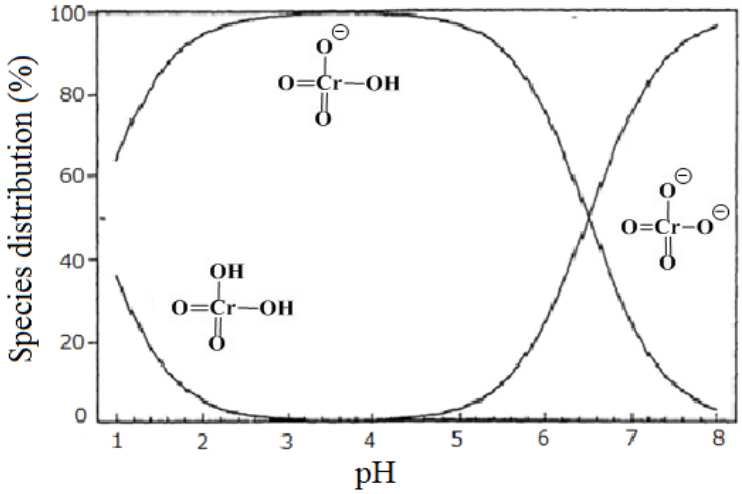

Fig. 2-4 Species distribution curves of Cr(VI) in environmental water.

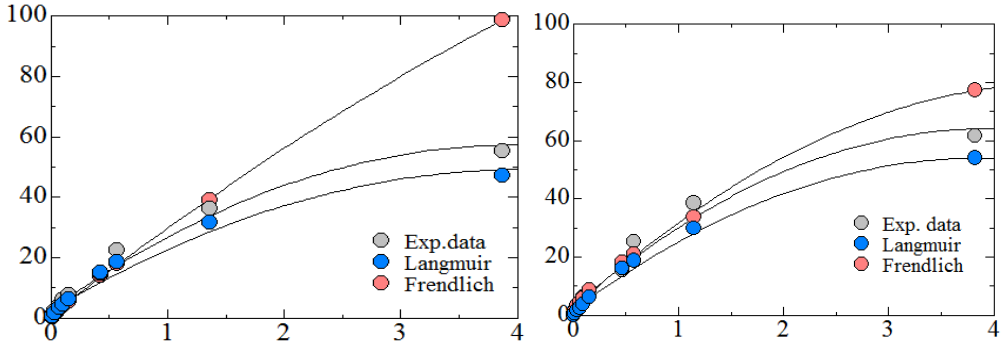

(a) **(b)**

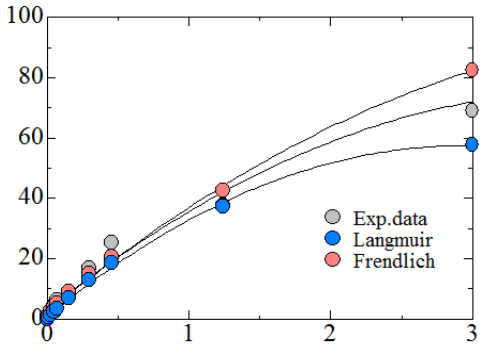

(c)

Fig. 2-5 Adsorption isotherm of Cr(VI) on (a) chitosan, (b) EP and (c) GA.

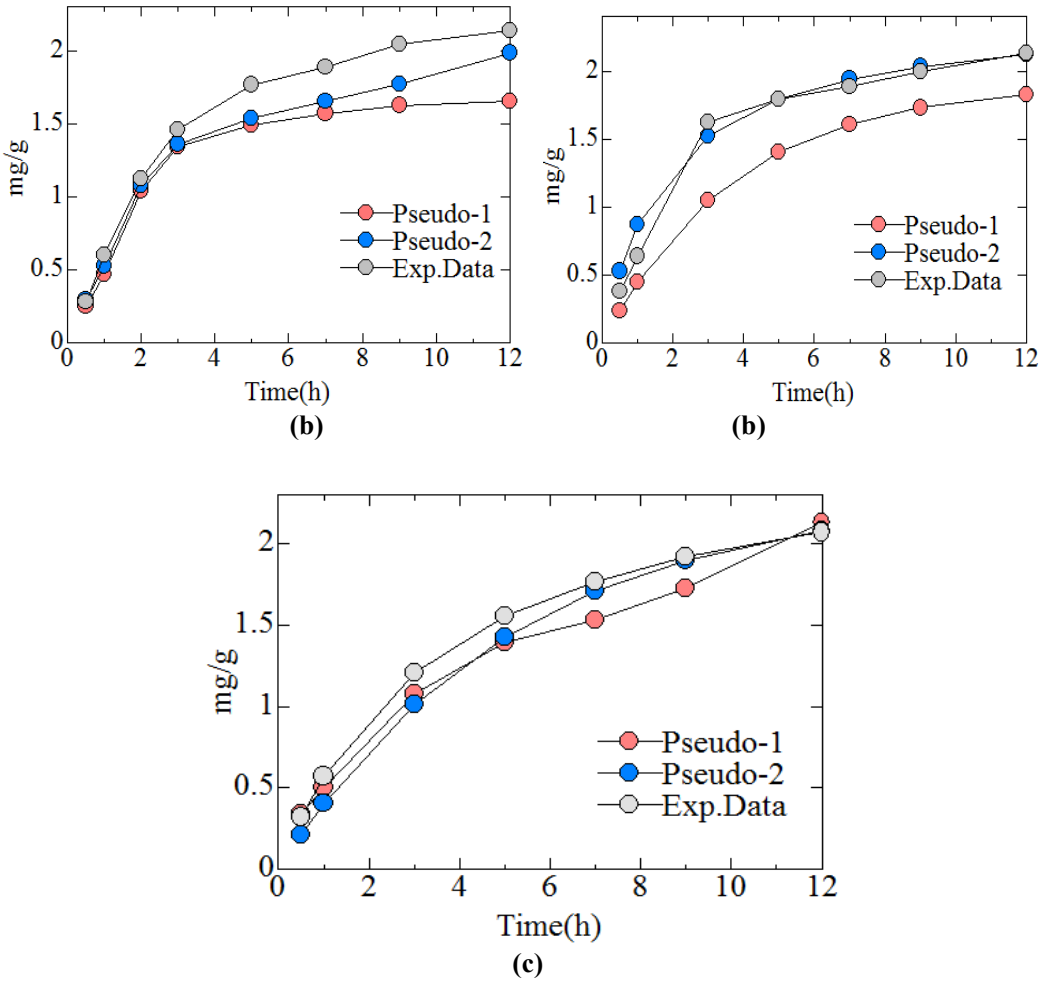

(b) (b)

(c)

Fig. 2-6 Adsorption kinetics of Cr(VI) on (a) chitosan, (b) EP and (c) GA.

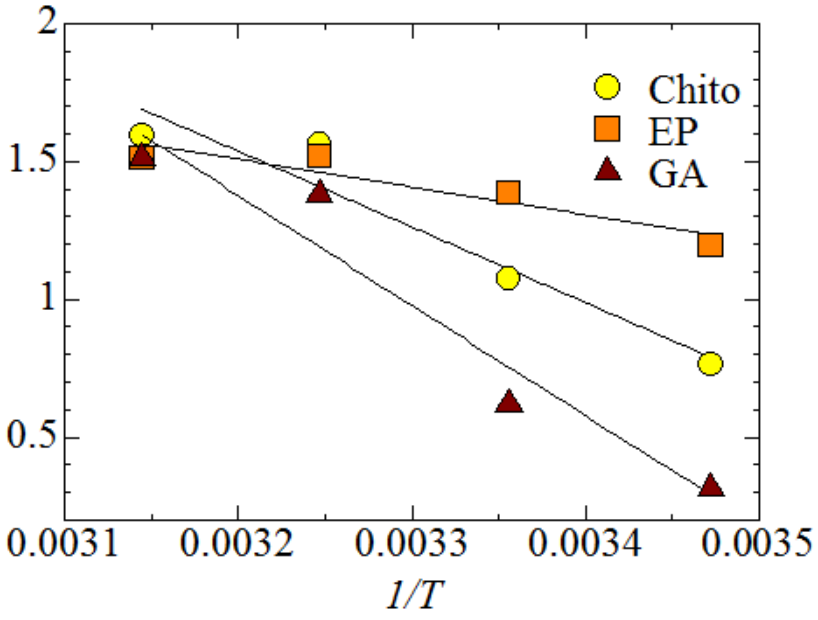

Fig. 2-7 The van't Hoff plot for different temperature.

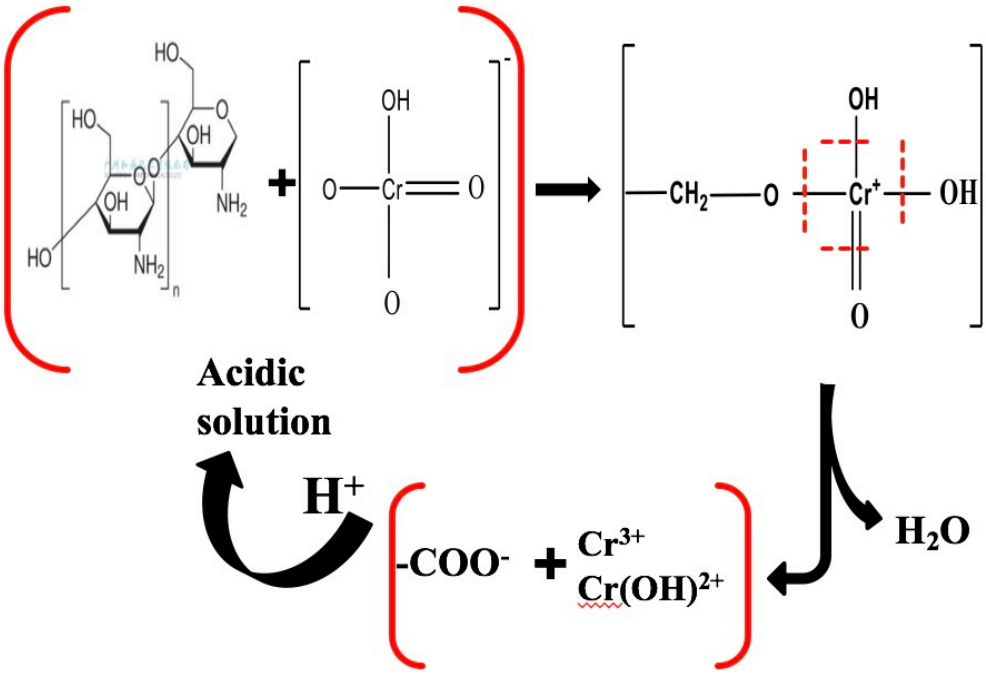

Fig. 2-8 The mechanism of Cr(VI) sorption on cross-linking chitosan.

Chapter 3 Removal of U(VI) Using the Cross-linked Chitosan

3. 1 Introduction

In recent years, environmental pollution is one of the most serious problems in the world. Thus, the monitoring, reduction and recovery of the harmful pollutants such as heavy metal in natural environment is very significant from the viewpoint of environmental protection.

Uranium is present in the environment as a result of leaching from natural deposits, discharge from mill tailings, emissions from the nuclear industry, combustion of coal and other fossil fuels, and use of uranium-containing phosphate fertilizers [88]. Naturally occurring uranium is a mixture of three radioisotopes (^{234}U, ^{235}U and ^{238}U), but majority of them are ^{238}U isotope (99.27%). Radioactive U(VI) can directly damage biological organization or produce reactive species, and it is a possible harmful pollutant in the environment. Particularly, the mining and milling of U minerals generate in large quantities of waste materials (tailings), which causes environmental health concerns. The maximum uranium level in drinking water recommended by the World Health Organization [89] is 15μg/L, and the maximum contaminant level set by the USEPA [90] for drinking water standard is 20μg/L.

Uranium (U) is known as the sources of nuclear power, and widely distributed in nature [91]. Radioactive U(VI) can directly damage biological organization or produce reactive species [92], and can be a possible harmful pollutant in the environment. Particularly, the mining and milling of U minerals generate in large quantities of waste materials (tailings), which causes environmental health concerns [93-96]. For the sake

of ecosystem stability and public health, it is necessary to decrease the concentration of U(VI) in contaminated groundwater to the permissible limits [97].

From above-mentioned, the chitosan and cross-linked chitosan were synthesized in this work to enhance the adsorption potential of U(VI). The aim of this paper is to investigate the adsorption efficiency of cross-linked for more practical use in the future. Adsorption isotherms of U(VI) was studied and analyzed using Langmuir and Freundlich equations, and kinetics analyses were also carried out.

3. 2 Experimental Sections

3. 2. 1 Materials and Reagents

Chitosan was prepared from purified natural shells of crustacean contained chitin about 30%. Chitosan was stirred with the acetic acid solution 200 ml (2.0%) and added drop-wise to 100mL of 0.5M NaOH.

Chitosan was added to 1.0wt% of EP, adjust the pH to 14. After keeping the mixed solution at 60 ℃ for 6h, we can get cross-linking with EP. Chitosan was added to 1.0wt% of GA, adjust the pH to 7. After keeping the mixed solution at room temperature for 24h, we can get cross-linking with GA.

Uranium standard solutions used for making the calibration curve were prepared by diluting the standard solutions (DWS-3; 20mg·dm^{-3} 2% HNO_3 solution) purchased from GL Sciences, Inc. (Japan). All other chemical reagents were also purchased from Kanto Chemical Co., Inc. All reagents used were of analytical grade, and water (>18.2 MΩ in electrical resistance) which was treated by an ultrapure water system (Advantec aquarius: RFU 424TA, Advantec Toyo, Japan) was employed throughout the work.

3. 2. 2 Experiment of Apparatus

The morphology of cross-linked chitosan was characterized by a SEM (JSM-5800, JEOL, Ltd.). The material was placed on a microgrid of silicon, and transferred to the analysis chamber in the SEM equipment.

The cross-linked chitosan was also investigated using FTIR spectroscopy (FTIR-4200, Jasco, Corporation) to identify the functional groups. For FTIR in pressed KBr pellets, the sample was washed three times with ethanol for 5 min, filtered, and dried at

110 °C for 24 h. The spectral resolution was set to 1 cm^{-1}, and 150 scans were collected for each spectrum.

The specific surface areas and pore volumes of cross-linked chitosan were measured by N_2 adsorption/desorption using a surface area and pore size analyzer (TriStar II 3020, Micromeritics, Instrument Corporation) after vacuum degassing of the sample in the tube at 200 °C for 12 h.

An ICP-MS (Inductively Coupled Plasma Mass Spectrometry) instrument (ThermoFisher Scientific X_2) was used to determine the concentration of U(VI).

3. 2. 3 Sorption Experiment of U(VI) Using Cross-linked Chitosan

The adsorption capacities of Cr from aqueous solution of the cross-linked chitosan were investigated by a batch method. Cross-linked chitosan was thoroughly mixed with 100 cm^3 of containing known amount of U(VI) in a 200 cm^3 conical flask, and the suspensions was shaken by an automatic shaker (PLUS SHAKER EP-1, TAITEC, Corporation) in a water bath at room temperature (25 ± 2 °C). Sorption experiments were conducted by varying the pH (1-8), contact time (0.5h-24h), sorbent dosage (0.1-0.5 $g \cdot dm^{-3}$). The pH of each solution was adjusted by using 0.1 $mol \cdot dm^{-3}$ NaOH and 0.1 $mol \cdot dm^{-3}$ HNO_3.

Adsorption isotherms of U(VI) onto cross-linked chitosan was measured at varying initial U(VI) concentrations (0.1-0.35 $mg \cdot dm^{-3}$) under optimized conditions.

Following each sorption experiment, the suspension containing cross-linked chitosan and the above standard solution was filtered through a 0.45 μm membrane filter (Advantec Mixed Cellulose Ester, 47 mm) to remove Cr(VI) that have been

adsorbed into the cross-linked chitosan. Then the concentration of this metal in the filtrate was determined with an ICP-MS. Replicate experiments were basically performed three times. The operating conditions of ICP-MS are shown in Table 3-1.

3. 3 Results and Discussion

3. 3. 1 Effect of pH

Solution pH is one of the most important parameters affecting adsorption characteristics. In order to investigate the effects of solution pH on the uptake of U(VI), sorption experiments were conducted at different pH values at room temperature 25 °C, while the concentration of U(VI) was kept constant at 100 ppb, and adsorbent dosage was 0.1g·dm^{-3}. The contact time was 5 h.

The results for U(VI) are shown in Fig 3-1, it can be seen that the adsorption capacity of Cr(VI) reaches maximum at pH 5 for the adsorbents, which is due to the changes of the surface charge of the adsorbent. The reason is as follows. Aqueous solution pH can affect the surface charge of the adsorbent, the degree of ionization, speciation of metal ions, and surface metal binding sites.

On the other hand, Fig 3-1 shows the pH dependence of hydrogen chromate anion distribution. U exists predominantly as monomeric species UO_2^{2+}, and small amounts of $UO_2(OH)^+$ at pH≤4.3, and at pH≥5 colloidal or oligomeric species, i.e. $(UO_2(OH)_2^{2+}$, $(UO_2)_3(OH)_5^+$, $(UO_2)_4(OH)_7^+$, $(UO_2)_3(OH)_7^-$ are formed [98-101].

From above-mentioned, it can be considered that the U(VI) adsorption occurred ominantly by cation exchange reaction between H^+ of hydroxyl groups on adsorbents and cationic species of U(VI). Then, pH 5 was taken for further experimental work, although the uptake of U(VI) maintains the highest level at pH 5-8.

3. 3. 2 Adsorption Isotherms

Adsorption isotherms are commonly used to reflect the performance of adsorbents in adsorption processes. In this paper, Langmuir and Freundlich isotherms were applied to the data obtained in this work. The linear plots of C_e and m were presented for Langmuir and Freundlich models, and the coefficient of both isotherms are shown in Table 3-2. From Table 3-3, it is also found that chitosan is more fitted to Langmuir isotherm, EP and GA compared to Chitosan, fitted to Frendlich as well as Langmuir. Adsorption isotherms of Cr(VI) on the modified chitosan can be generally described by Langmuir isotherm more satisfactorily. The adsorption may have occurred mainly by monolayer reaction.

From Table 3-2, the maximum adsorption capacity of modified chitosan reached 717 μg/g from 223 μg/g by cross-linked with EP under our experimental conditions. That is to say, modified chitosan by cross-linking can be an efficient adsorbent for U(VI).

3. 3. 3 Kinetic Studies

When we added the adsorbents 0.20g/L, U(VI) 100μg/L, adjusted pH was 5. From Fig 3-3 and Table 3-3, 3-4, 3-5 the rates of adsorption by modified chitosan were found to more conform to pseudo-second order kinetics. The rates of adsorption using the modified chitosan for the removal of U(VI) were found to conform to pseudo-second order kinetics.

3. 3. 4 Mechanism of U(VI) sorption on cross-linking chitosan.

Chitosan can be an excellent biosorbent for metals because its amine ($-NH_2$) and hydroxyl (-OH) groups may serve as coordination sites to form complexes with various

heavy metal ions. In order to increase the number of exposed active sites, regard to chitosan cross-linked EP, amino groups of chitosan were not damaged during the process of cross-linking because EP are mainly associated with hydroxyl groups. In the case of chitosan cross-linked GA, the reaction of Schiff base between the aldehyde group of GA and the amido of chitosan is dominant. The mechanism of U(VI) sorption on cross-linking chitosan as shown in the Fig 3-4.

3. 4 Conclusions

The efficiency of cross-linked chitosan as an adsorbent for U(VI) was investigated. From this work, the following matters were clarified:

(1) The uptake of U(VI) was performed even at pH 1-3 by cross-linking. The adsorption capacity of U(VI) reached maximum at pH 5 for the adsorbents.

(2) The maximum adsorption capacity of modified chitosan reached 717 μg/g from 223 μg/g by cross-linking with EP under our experimental conditions.

(3) Adsorption isotherms of U(VI) on the modified chitosan can be generally described by Langmuir isotherm more satisfactorily. The adsorption may have occurred mainly by monolayer reaction.

(4) The rates of adsorption using the modified chitosan for the removal of U were found to conform to pseudo-second order kinetics.

From these results, it was quantitatively clarified to some extent that cross-linked chitosan can be an efficient sorbent for U(VI), which provide very significant information from the viewpoint of environmental protection.

Tables

Table 3-1 Operating conditions of inductively coupled plasma mass spectrometry (ICP-MS).

RF power	1400 W
Plasma gas flow	15 l·min^{-1}
Carrier gas flow	1.2 l·min^{-1}
Sampling depth	6.5 mm
Sample uptake rate	0.5 ml·min^{-1}
Measurement point	3 points/peak
Integration time	1.0 sec/point
Measured isotope	^{238}U

Table 3-2 Coefficient of Langmuir and Freunndlich isotherms for U(VI)

	Langmuir isotherm			**Freundlich isotherm**		
	Q_m[$\mu g/g$]	K_L[$L/\mu g$]	R^2	b_F	K_F [$\mu g/g$]	R^2
Chitosan	223	0.102	0.785	0.0987	89.7	0.632
EP	717	0.291	0.996	0.211	162	0.986
GA	685	0.212	0.987	0.186	98.1	0.964

Table 3-3 Pseudo-first or second-order model kinetic parameters of U(VI) on chitosan

	Pseudo-first-order model	Pseudo-second-order model	
K_1(h^{-1})	0.140	K_2(g/mg h)	0.288
q_e (mg/g)$_{cal}$	2.121	q_e (mg/g)$_{cal}$	2.127
R^2	0.887	R^2	0.999

Table 3-4 Pseudo-first-order model kinetic parameters of U(VI)

	Chitosan	EP	GA
K_1(h^{-1})	0.140	0.211	0.151
q_e (mg/g)$_{cal}$	2.121	2.31	2.42
R^2	0.887	0.983	0.941

Table 3-5 Pseudo- second-order model kinetic parameters of U(VI)

	Chitosan	EP	GA
K_2(g/mg h)	0.288	0.334	0.301
q_e $(mg/g)_{cal}$	2.127	2.66	2.81
R^2	0.999	0.996	0.987

Figures

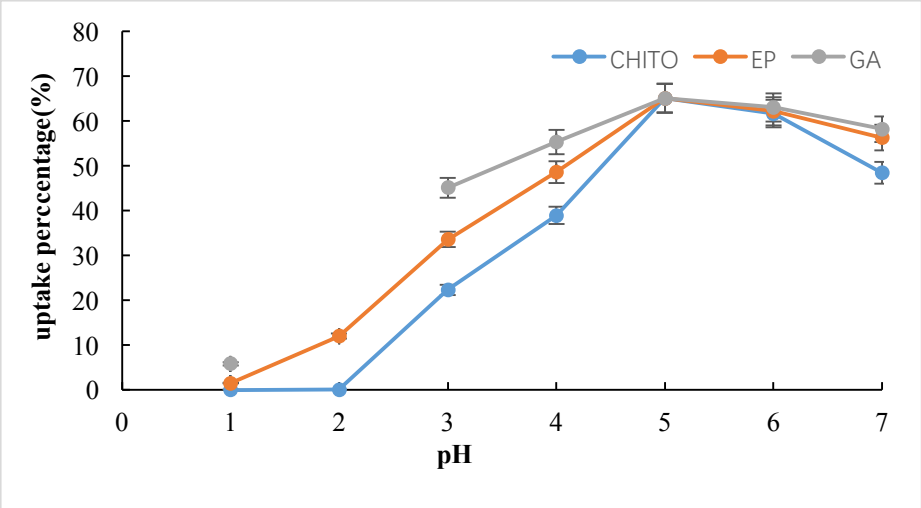

Fig. 3-1 Effect of pH on percent removal of U using chitosan, EP and GA.

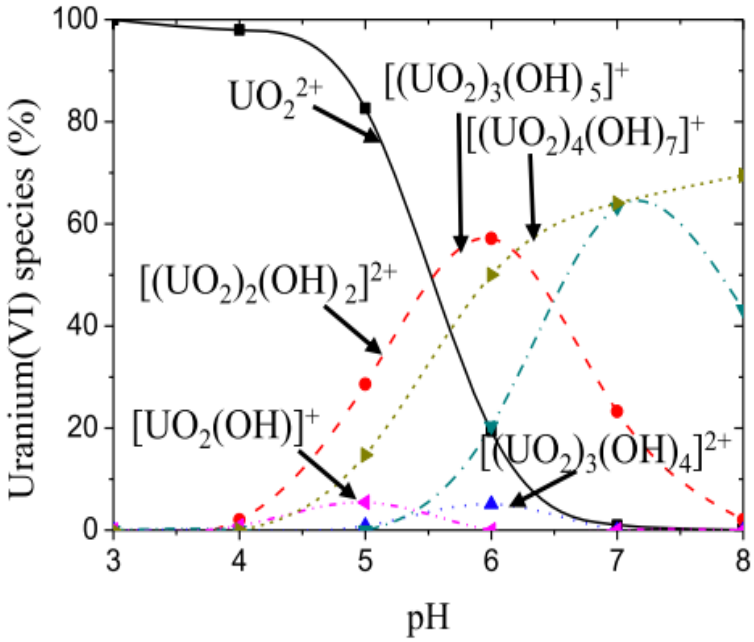

Fig. 3-2 Species distribution curves of U(VI) in environmental water.

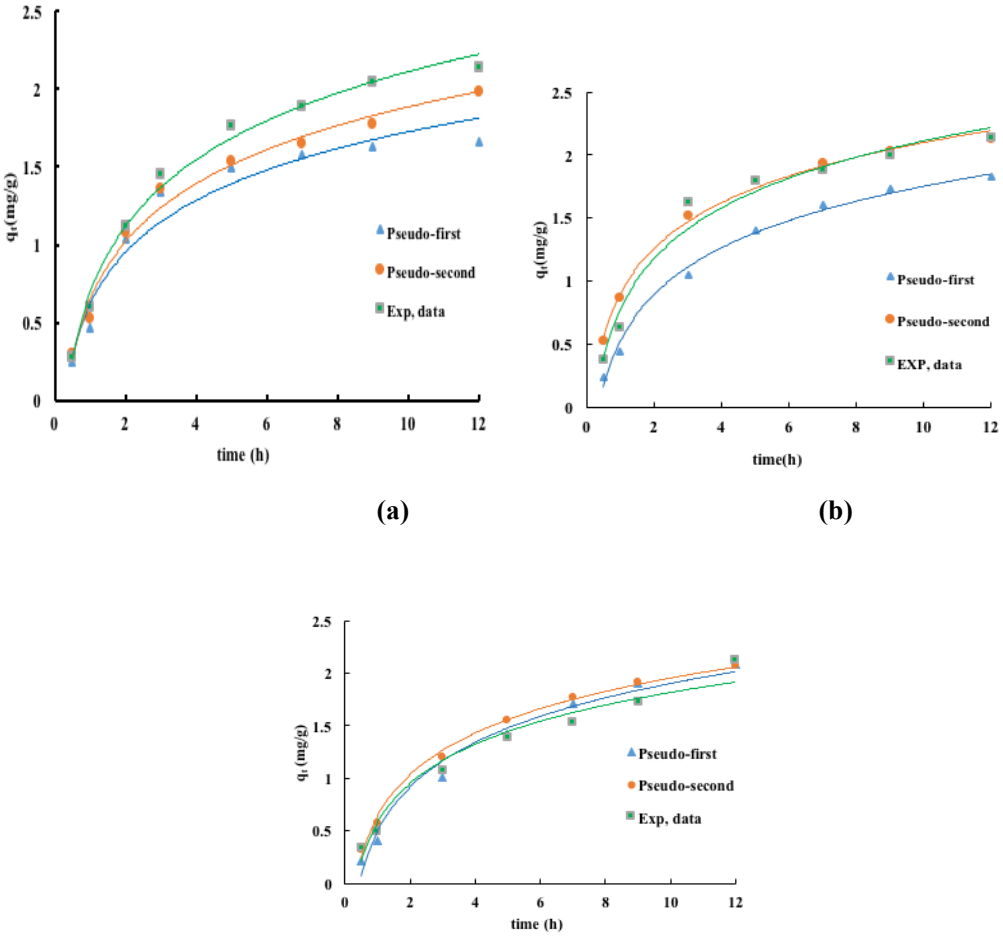

Fig. 3-3 Adsorption isotherm of U(VI) on (a) chitosan, (b) EP and (c) GA.

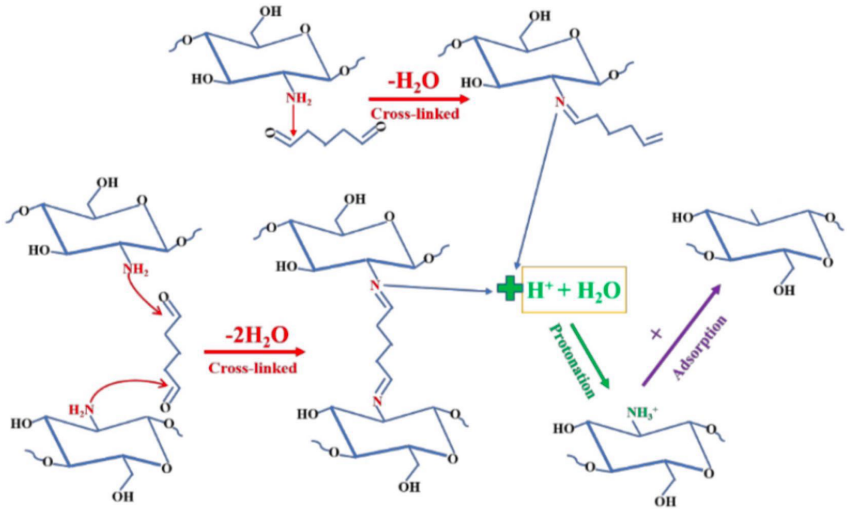

Fig. 3-4 Mechanism of U(VI) sorption on cross-linking chitosan.

Chapter 4 Removal of Cr(VI) Using the Sodium Dodecyl Sulfate (SDS) modified with chitosan

4. 1 Introduction

It is well known that investigations examining the abundant levels of toxic heavy metal ions discharged to the environment have now received considerable attention. One of the compelling reasons for this is the fact that these ions pollute air, soil, and water, thus having a great effect on human health [102,103]. Chromium (Cr) is the first element in transition metal of group VIB in the periodic table [104].

They can be taken up by plants and easily be leached out into the deeper soil layers, leading to ground and surface water pollution. Because of its high toxicity and its water solubility in the full pH range. The effluents are discharged onto the open land or into the sewage system. These industries are major sources of chromium pollution in the environment [105]. Cr(VI) must be substantially removed from the wastewater before being discharged into the aquatic system.

Many works for the removal of heavy metals by adsorption has been reported [106-107]. Particularly, the development of high efficiency and low cost adsorbents has been aroused general interest in recent years. Chitosan has free amino groups and hydroxyl groups, which can remove the heavy metal ions by forming stable metal chelates.

However, chitosan had some defects such as notable swelling in aqueous media and nonporous structure resulting in a very low surface area [108]. Therefore, many types of chemical modification can be undertaken to produce some chitosan derivatives for improving the removal efficiency of the heavy metal.

In this work, we evaluated the adsorption of chitosan modified with sodium dodecyl sulfate (SDS) as part of the adsorption study of Cr using modified chitosan. It has been reported that SDS-modified chitosan beads can be used to remove cationic dyes [90]. The aggregation of particles through a bridging structure can be described as a two-step pathway: 1) initial chain adsorption and bridging, followed by 2) floc maturation/reconfiguration. Before the interparticle connection occurs, the chain of SDS must be adsorbed on a chitosan surface [48]. Furthermore, chitosan modified with SDS has recently been used for the removal of heavy metals, such as cadmium [49,50]. However, the use of SDS-modified chitosan as an adsorbent of Cr with varying initial concentrations of SDS for optimizing the adsorbent has rarely been evaluated. The objective of the present research was to investigate the efficiency of SDS-modified chitosan beads as a sorbent for Cr(VI) for more practical uses in the future, and to reveal the adsorption mechanism.

From above-mentioned, the SDS modified with chitosan was synthesized in this work to enhance the adsorption potential of Cr(VI). The adsorption capacity of the hybrid membrane was investigated for the removal of Cr(VI) from aqueous solution under varying experimental conditions.

4. 2 Experimental Sections

4. 2. 1 Materials, Reagent and Apparatus

Chitosan and sodium dodecyl sulfate (SDS; M.W.: 288.372 g/mol) were purchased from Tokyo Chemical Industry Co., Inc. Cr(VI) standard solutions were prepared by diluting a standard solution (1,000 mg·dm^{-3} $K_2Cr_2O_7$ solution) purchased from Kanto Chemical Co., Inc. Acetic acid, NaOH, HNO_3, $NaSO_4$, ethylenediaminetetraacetic acid disodium salt dihydrate, and toluene, were obtained from Kanto Chemical Industry Co., Inc. All other chemical reagents were also bought from Kanto Chemical Co., Inc. All reagents used were of analytical grade, and water (>18.2 MΩ in electrical resistance) which was treated by an ultrapure water system (Advantec aquarius: RFU 424TA, Advantec Toyo, Japan), was employed throughout the work.

The pH of Cr(VI) aqueous solution were measured by the pH meter (HORIBA UJXT 06T8, Japan). The surface property of SDS modified chitosan was characterized by SEM (JEOL, JSM-5800, Japan), XPS (ESCALAB 250 Xi, Japan) and Fourier transform infrared spectroscopy in pressed KBr pellets (FTIR-4200, Jasco, Japan). The concentrations of Cr(VI) in solution were determined by ICP-AES (inductively coupled plasma atomic emission spectrometry).

4. 2. 2 Prepared chitosan modified with SDS

1.5 g of chitosan was placed in acetic acid solution (2.0%), and the solution was mixed 24 h. The chitosan-gel was prepared by dropping the above chitosan solution into 200 mL of 0.20 mol·dm^{-3} NaOH. The obtained gel was rinsed with ultrapure water until attaining a pH of 7 after stirring for 24h. Subsequently, 200 tablets of chitosan-gel

beads were placed in 100 mL SDS solution (including the fixed concentration of SDS), and then left for five days. Therefore, chitosan-gel beads modified with SDS were obtained. Finally, the SDS-modified chitosan beads were dried at 60 ℃ overnight for their use as an adsorbent.

4. 2. 3 Sorption Experiment of Cr(VI) Using SDS-chitosan beads

The adsorption capacities of Cr(VI) from aqueous solution using the SDS-chitosan beads was investigated by a batch method. SDS-chitosan beads was thoroughly mixed with 50 ml of containing known concentrations of Cr(VI) in a 200 ml conical flask. According to the above-mentioned procedure, Cr(VI) were adsorbed at different pH values (1-7), contact time (1-96h), SDS initial concentration of 10-9000 $mg \cdot dm^{-3}$ and sorbent dosage (0.01-0.06 $g \cdot dm^{-3}$). The pH of each solution was adjusted by using 0.1 $mol \cdot dm^{-3}$ NaOH and HNO_3.

4. 3 Results and Discussion

4. 3. 1 Characteristics of SDS-chitosan beads

The SEM-EDS images of chitosan beads and SDS-chitosan beads (40 mg/L SDS loading) are shown in Fig 4-1. From SEM images, it could be determined that the diameter of these beads was roughly 800 μm. These figures show that the surface of the membrane appears concave and convex. This may be attributable to the loss of water (about 98%) contained in the sorbent upon the drying of chitosan. It is considered that adsorption proceeded with physical and chemical adsorption. The mapping images show that Cr ions were satisfactory adsorbed on the adsorbent.

The FT-IR spectra of the chitosan and SDS-chitosan beads are exhibited in Fig 4-2. The broad and intense peak at 3400 to 3500 cm^{-1} corresponds to O-H and -NH_2 stretching vibrations of hydroxyl groups of chitosan and SDS-chitosan [83-85]. The peak at 2871 cm^{-1} is related to the aliphatic methylene group . The wide peaks at 1560 to 1640 cm^{-1} and 1110 cm^{-1} show the imine group and ether group [86]. The SDS-modified chitosan bands at around 1248 cm^{-1} are characteristic of the asymmetrical vibrations of the C-O-S group [109,110]. The adsorbent could be identified as a composite of SDS and chitosan.

XPS analysis was employed to survey the chemical compositions and binding condition of the surface on samples. Chitosan beads with different amounts of SDS loading were analyzed (Fig 4-3 (a): Chitosan, (b): SDS100-chitosan, (c): SDS600-chitosan, and (d): SDS6000-chitosan). As can be seen in Fig 4-3, the C1s spectra of these samples displayed peaks at 284.5 eV and 286.5 and 288.5 eV, corresponding to

C-C bonds C-O and C＝O, respectively. It also shows that the S 2p spectra of SDS600-chitosan and SDS6000-chitosan displayed peaks at 169 eV. From Table 4-1, it could be found that the predominant elements were carbon and oxygen, and that the SDS100-chitosan and SDS600-chitosan atomic values of the N element are 1.75% and 1.69%, respectively. The SDS600-chitosan and SDS6000-chitosan atomic values of the S element are 2.78% and 6.85% respectively, which suggests that the higher the concentration of loading SDS is, the higher the concentration of the S element is.

4. 3. 2 Effect of pH

The solution pH is one of the most important parameters in the adsorption process. The effect of the pH on Cr(VI) adsorption by SDS-modified chitosan beads is shown in Fig 4-4. In this experiment, the shaking time was 24 hours, temperature was 25 ℃, dose of adsorbent was 0.02 g/L, and initial Cr(VI) concentration was 1 mg/L. The acidity of the solution had a significant effect on the adsorption of SDS-modified chitosan beads towards Cr(VI), where the amino groups of chitosan were protonated and positively charged. Moreover, the sulfate group is a typical strong acid group. Therefore, even under the acidic condition, which would not easily hydrolyze with water, surfactants could behave fully in their anionic form. As everyone knows that chitosan molecules are protonated at amino groups which carry cationic adsorption sites and are dissolved in the acidic region [48]. Apart from cationic amino groups, chitosan chain adsorption (leading to interparticle bridging) can also occur through hydrogen bonds [88]. Similar to cationic polyacrylamide, chitosan is thus able to aggregate anionic soluble compounds (through electrostatic affinities) and simultaneously

flocculate particulate matter through interparticle bridging mechanisms. However, the protonation of amino groups (i.e., the effective charge density of the chitosan polymer chain) can be influenced by the pH [48]. It makes impossible to conduct adsorption experiments at pH levels of 1-3. The factor of pH on the adsorption of Cr(VI) by SDS-modified chitosan beads was estimated by adjusting the pH in the range of 4 to 10 (Figure 3). The maximum uptake of Cr(VI) ions took place at pH 4-5, which may be attributable to the converts in the surface charge of the adsorbent. With an increase of the pH at above pH 5, the uptake decreased.

Cr(VI) may be present in the form of $HCrO_4^-$ and CrO_4^{2-}. As shown in Fig 2-2, $HCrO_4^-$ is dominant in the pH range of 2-4. However, CrO_4^{2-} becomes increasingly dominant as the solution becomes more basic, and the form of CrO_4^{2-} becomes stable above the pH of 7 [49]. The process of shifts is given by the following equations:

$$HCrO_4^- \leftrightarrow CrO_4^{2-} + H^+ \qquad pKa = 5.9 \qquad (4\text{-}1)$$

$$H_2CrO_4 \leftrightarrow HCrO_4^- + H^+ \qquad pKa = 4.1 \qquad (4\text{-}2)$$

$$Cr_2O_7^{2-} + H_2O \leftrightarrow 2HCrO_4^- \qquad pKa=2.2 \qquad (4\text{-}3)$$

As a result of this, the functional groups combining with chromate ions may decrease due to the increase of their ion valence. It is supposed that amino acids with a positive charge combine with hydroxyl ions after binding with protons. Therefore, the adsorption capacity can largely depend on the kinds of functional group and the existing form of Cr (VI). The surface of the SDS-chitosan beads became positively charged owing to strong protonation in these pH ranges, which led to a stronger attraction between the positively charged surface and the negatively charged $Cr_2O_7^{2-}$ and $HCrO_4^-$.

4. 3. 3 Effect of Contact Time

The effect of the contact time on the adsorption capacity of Cr(VI) by SDS-modified chitosan beads was explored. In this experiment, the concentration of Cr(VI) was set as 1 mg/L with the dose of 0.05 g at a temperature of 25 °C. The pH of the solution was kept at 4, in order to achieve the maximum removal of Cr(VI). As can be seen from the Fig 4-5, the results with varying contact times from 1 to 96 h.

The adsorption capacity of SDS-chitosan beads for Cr(VI) increased sharply within the first 24 h, which may be attributable to the availability of the sites on the surface of adsorbent. It is suggested that a concentration gradient is present both the adsorbent and adsorbate in the solution [50]. Then, it reached adsorption equilibrium at 72 h, and further more, there was no appreciable increase (Fig 3-5). Therefore, the optimized contact time was taken to be 72 h for further studies. The surface modification of the chitosan beads by SDS facilitates the adsorption through an ion-exchange mechanism [38]. Usually, the complexation mechanisms involve slower kinetics than the ion-exchange and hydrogen bonding reaction mechanism [81-83].

4. 3. 4 Effect of adsorbent dosage

To determine the effect of the adsorbent dosage on the removal of Cr(VI), the experiments were carried out by varying the dosage (from 0.4 to 1.0 mg/L) and keeping all other parameters constant (temperature: 25 °C; pH: 4; contact time: 24 h; initial concentration: 1.0 mg/L). The results are shown in Fig 4-6. The removal of more than 80% Cr(VI) was observed for the 0.8 mg/L dosage, but no extraordinary increase was observed at a dosage of more than 0.8 mg/L. Therefore, 0.8 mg/L was regarded

compose the optimum dosage for the removal of Cr(VI) in this study. A higher dose provides a larger number of binding sites, which eventually causes the enhanced removal of Cr(VI).

4. 3. 5 Effect of coexisting ions

The effect of competitive anions on the adsorption of Cr(VI) is shown in Fig 4-7. In this experiment, the initial concentration of Cr(VI) was set as 1 $mg \cdot dm^{-3}$. These counter ions were tested collectively, and all various ions were included at 50, 100, or 200 mg/L in solution. From this figure, the removal of Cr(VI) was remarkably decreased under the presence of common ions at above 50 $mg \cdot dm^{-3}$ (i.e., 50 times the Cr(VI) concentration or more), although no large decrease was observed when the concentration of each common ion was below 10 $mg \cdot dm^{-3}$ in our former preliminary experiments. Both Cr (VI) and other competitive anions may be attracted to the amino group by the electrostatic force. Therefore, Cr(VI) was shown to be inhibited by adsorption when the concentrations of coexisting ions were large.

4. 3. 6 Estimation of partition coefficient (PC)

Many studies have shown that, the adsorption performance is usually evaluated and expressed by the maximum (or equilibrium) adsorption capacity. However, the maximum adsorption capacity is sensitively affected by the initial concentration of target pollutant (or more specifically, what is left after the sorption reaction) [111,112]. When the sorbent is exposure to a higher concentration of goal targets, it is likely to exhibit a higher adsorption capacity. On the other hand, when the sorbent is exposed to lower levels of target species, it will show lower capacities. Therefore, in addition to

the maximum adsorption capacity, it is effective to estimate using the concept of the partition coefficient (PC = adsorption capacity/final concentration) [53,54]. Comprehensived experimental data of the adsorption process under different effect factors are shown in Table 4-2. From Table 4-2, it could be found that the adsorption affinity was fairly good under the following conditions when using either the concept of the adsorption capacity or that of the PC: pH of 4-5, contact time of 72 h, initial concentration of SDS 40 $mg \cdot dm^{-3}$, and adsorbent dose of 0.8-1.0 $mg \cdot dm^{-3}$.

4. 3. 7 Adsorption Isotherms

Adsorption isotherms of Cr(VI) on SDS-chitosan beads were studied with varying initial concentrations from 0.010 to 3.0 mg/L under optimized conditions in terms of the pH (pH 4), contact time (72 h), and dosage of the adsorbent (0.8 mg/L) at 298 K in this work. Adsorption isotherms are generally used to reflect the performance of adsorbents in adsorption processes. Herein, two common adsorption models, consisting of Langmuir and Freundlich equations, were employed to explain the adsorption of Cr by SDS-chitosan beads (Fig 4-9, 4-10,4-11). The adsorption data acquired for Cr(VI) using SDS-chitosan beads were investigated by Langmuir and Freundlich equations, and the results are shown in 4-10 and 4-11, respectively. All isotherm parameters calculated from the two models are listed in Table 4-3, along with the correlation coefficients (R^2). High correlation coefficients indicate that Cr(VI) sorption can be well-described by the Langmuir and Freundlich isotherms. In particular, the Langmuir model was preferable, and the maximum adsorption capacity was estimated to be 3.23 mg/g. It is obvious that the Langmuir isotherm model elucidates the monolayer

adsorption on homogeneous surfaces. The results implied that the adsorption of Cr(VI) was a monolayer coverage process [113]. This indicated a strong potential in the application of SDS-chitosan beads for Cr(VI) removal from an aqueous phase. On the other hand, it was found that the R^2 value obtained from the Freundlich model was not small, and favorable adsorption was suggested, judging from the value of 1/n [114]. The isotherm parameters revealed that the SDS-chitosan bead with special structures could efficiently improve the adsorption capacities.

4. 3. 8 Kinetic Studies

An adsorption kinetics study was conducted to explore the relationship between the adsorption amount qt and time t. According to Fig 4-12, the adsorption content of Cr(VI) by SDS-chitosan beads increased significantly within 96 h. The quick adsorption within the initial 24 h indicated that attract Cr(VI) was mainly guiding by chemical sorption or surface complexation. This might be associated with the abundant exposure of sorption sites on the adsorbent surface. As the sorption sites were gradually occupied by Cr(VI), the absorb rate of Cr(VI) became slower with a lapse of time and ultimately approached equilibrium [115,116].

In the interest of comprehend the adsorption kinetics in more detail, the pseudo-first-order, pseudo-second-order, and intraparticle diffusion kinetic models were applied to simulate the kinetic sorption process [117,118]. The fit theory of pseudo-first-order and pseudo-second-order models are illustrated in Fig 4-13 and Fig 4-14, respectively. The calculated parameters, along with the correlation coefficient (R^2) of the two models, are listed in Table 4-4. The adsorption kinetics based on the

experimental values were both in good agreement with the pseudo-first-order and pseudo-second-order kinetic models judging from the high correlation coefficients. The fitness of the pseudo-first-kinetic model implied that the rate-controlling step might involve chemisorption or chemical bonding between Cr(VI) and the functional groups of adsorbents. However, the rapid phase in the initial step of the adsorption process may involve physical adsorption or exchange at the adsorbent surface [84,119]. Although the adsorption data could be well-described by the pseudo-first-kinetic model, the diffusion of Cr(VI) into pores could play an important role for Cr(VI) adsorption on the adsorbent, since SDS-chitosan beads are porous structures. Therefore, an intraparticle diffusion model was also employed to elucidate the diffusion mechanism and to investigate whether the film or pore diffusion was the controlling step in the adsorption process. The plots of qt versus $t^{1/2}$ for the adsorption of Cr(VI) fitting as an intraparticle diffusion model are provided in Fig 4-15. From this figure, it is revealed that plural processes influence the adsorption process for the adsorption of Cr(VI) by SDS-chitosan beads. In the pseudo-first-kinetic model, the adsorption rate was very high. This may be attributed to the film diffusion of Cr(VI) through the hydrodynamic layer to the surface of SDS-chitosan beads and the diffusion of Cr(VI) through the boundary layer to the external surface of the adsorbent. As the adsorption on the external surface reaches saturation, Cr(VI) molecules can enter into the pores of the adsorbent and be adsorbed on the internal surface of the mesopores. It is considered that the intraparticle diffusion starts to slow down and reaches an equilibrium stage with the lessen of the Cr(VI) concentration in solution [89, 120].

4. 3. 9 Thermodynamic study

The adsorption experiments of Cr(VI) were carried out from 288 to 318 K for the thermodynamic investigation. The Gibb's free energy change (ΔG), enthalpy change (ΔH), and entropy change (ΔS) were calculated from the adsorption isotherms at different temperatures. All of the thermodynamic parameters for the adsorption of Cr(VI) on SDS-chitosan beads are tabulated in Table 4-5, and the adsorption capacity of Cr(VI) depending on the temperature is shown in Fig 4-16. The negative values of ΔG suggest the preferred occurrence of spontaneous adsorption over the tested temperatures (288 to 318 K). As shown in Figure 18, the adsorption capability of Cr(VI) on SDS-chitosan beads increased with an increase of temperature. In addition, the minus value of ΔG increased with the increase of temperature. This indicates that the adsorption of SDS-chitosan beads on Cr(VI) is more favorable at a higher temperature. Besides, the enthalpy ΔH of SDS-chitosan beads (ΔH > 0) denoted the endothermic adsorption reaction, with the probable better adsorption results at a high temperature. It is known that the value of ΔG is between 0 and -20 kJ/mol for physisorption, and that it is between -80 and -400 kJ/mol for chemisorption [121]. In certain conditions, the physisorption and chemisorption can be classified by the magnitude of ΔH and ΔG. Bonding strengths of < 84 kJ/mol are typically considered as those of physisorption interaction [122]. Then, it is suggested that the adsorption of Cr(VI) on SDS-chitosan beads can be mainly dominated by physisorption judging from the values of ΔH and ΔG.

4. 3. 10 Mechanism of Cr(VI) sorption on SDS-Chitosan Beads

In this study, SDS is loaded onto chitosan beads, and the prepared adsorbent will have a bilayer of SDS over the surface of pure chitosan beads as shown in Fig 4-17 judging from the literature [102]. That is, the role of SDS is to enhance the ion capturing capacity (i.e., to enhance the adsorption of Cr(VI)).

4. 4 Conclusions

The efficiency of SDS-chitosan beads as an adsorbent for Cr(VI) was investigated. According to these studies, the following conclusions were clarified:

(1) The optimal conditions of adsorption Cr(VI) using SDS-chitosann was determined. The optimal pH is pH 4; the optimal initial SDS concentrations is 40 mg/L; the optimal dosage is 0.8g.dm^{-3} and contact time was 72h considered as optimum initial concentration.

(2) The results showed that the maximum adsorption capacity and partition coefficient (PC) of Cr(VI) on SDS modified chitosan beads was 3.23 $mg \cdot g^{-1}$ and 9.5 $mg \cdot g^{-}1 \cdot mM^{-1}$, respectively.

(3) The best fit was obtained with a pseudo-second order kinetic model while investigating the adsorption kinetics.

According to the above conclusions, the results show that it the SDS-chitosan beads synthesized in this work can be effectively utilized for removing Cr(VI) ions. It is very significant information from the viewpoint of environmental protection, and can be used for treating industrial wastewaters including pollutants.

Tables

Table 4-1 Atomic ratio of each chitosan bead obtained by XPS analysis.

Name / Atomic%	Chitosan	SDS100 -chitosan	SDS600 -chitosan	SDS6000 -chitosan
Si 2p	4.41	2.06	0.81	
S 2p			2.78	6.85
C 1s	77.1	76.52	75.91	67.66
Cl 2p3	3.94	3.55		
Ca 2p	0.27	0.33	1.1	
N 1s		1.75	1.69	
O 1s	14.27	15.78	14.34	20.19

Table 4-2 Detailed experimental data of the adsorption process under different effect factors.

Target Ions	Adsorbent	Effect Factor	Final Concentration ($\mu g \cdot L^{-1}$)		Adsorption Capacity ($\mu g \cdot g^{-1}$)	Adsorption Capacity/ Final Concentration(PC) ($\mu g \cdot g^{-1} \cdot \mu M^{-1}$)
Cr(VI)	SDS	pH	4	966.69	1665.39	0.034
			5	966.37	1681.62	0.035
			6	970.3	1484.99	0.031
			7	970.24	1488.23	0.031
			8	977.8	1114.81	0.022
			9	993.55	322.60	0.0065
			10	999.29	35.87	0.00071
		Contact time (h)	3	982.28	354.31	0.018
			9	974.53	509.35	0.026
			12	969.69	606.23	0.031
			24	957.04	859.12	0.045
			48	948	1039.91	0.055
			72	945.51	1089.86	0.058
			96	945.50	1090.21	0.058
		Initial Concentration of SDS ($mg \cdot L^{-1}$)	0	985	300	0.015
			10	955.93	881.49	0.046
			20	954.67	906.69	0.047
			40	952.63	947.37	0.050
			80	954.25	915.02	0.048
			100	955.20	896.11	0.047
			200	957.41	851.81	0.044
			600	962.73	745.33	0.039

	1000	963.44	731.16	0.038
	0.4	800	500	0.4
Dose	0.6	646.6	589	0.86
($mg \cdot L^{-1}$)	0.8	434.4	707	1.93
	1.0	292	708	2.42

Table 4-3 Coefficient of isotherms parameters for U(VI) using SDS-chitosan beads.

Metal	T(℃)	Langmuir isotherm			Freundlich isotherm		
		$Q_{max}(mg/g)$	R_L	R^2	$K_F(mg/g)$	$1/n$	R^2
Cr(VI)	25	3.23	0.308×10^{-4}	0.960	3.01	0.700	0.921

Table 4-4 Coefficient of kinetic parameters for U(VI) using SDS-chitosan beads.

Adsorbent	Pseudo-first-order model				Pseudo-second-order model		
	q_e (P-mg/g)	q_e (P-mg/g)	k_1 (min^{-1})	R^2	q_e (P-mg/g)	k^2 (g/mg · min^{-1})	R^2
SDS40	1.09	1.04	0.0610	0.997	1.26	0.0718	0.994

Table 4-5 Thermodynamic parameters for the adsorption of Cr(VI) on SDS-modified chitosan beads

T(K)	ΔH(kJ/mol)	ΔS(J/mol)	ΔG(kJ/mol)
288	80.70	288.18	-2.34
298	-	-	-5.22
308	-	-	-8.10
318	-	-	-10.98

Table 4-6 The comparison of adsorption properties of several adsorbents.

Materials	Initial Concentration ($mg \cdot L^{-1}$)	Final Concentration ($mg \cdot L^{-1}$)	Adsorption Capacity ($mg \cdot g^{-1}$)	Partition Coefficient ($mg \cdot g^{-1} \cdot mM^{-1}$)	Reference
Magnetic Chitosan	100	30.6	69.4	2.3	[14]
Carboxymethyl Chitosan-Silicon Dioxide	500	39.9	80.7	2.1	[30]
Chitosan-g-poly/silica	1000	44.3	55.7	1.3	[77]
Crosslinked chitosan bentonite composite	500	210.87	89.1	0.42	[78]
Graphene oxide/chitosan	200	13.8	86.2	6.2	[79]
Ethylenediamine-magnetic chitosan	500	148.2	51.8	0.35	[80]
Chitosan	1	0.85	1.60	1.9	This study
SDS-chitosan	1	0.34	3.23	9.5	This study

Figures

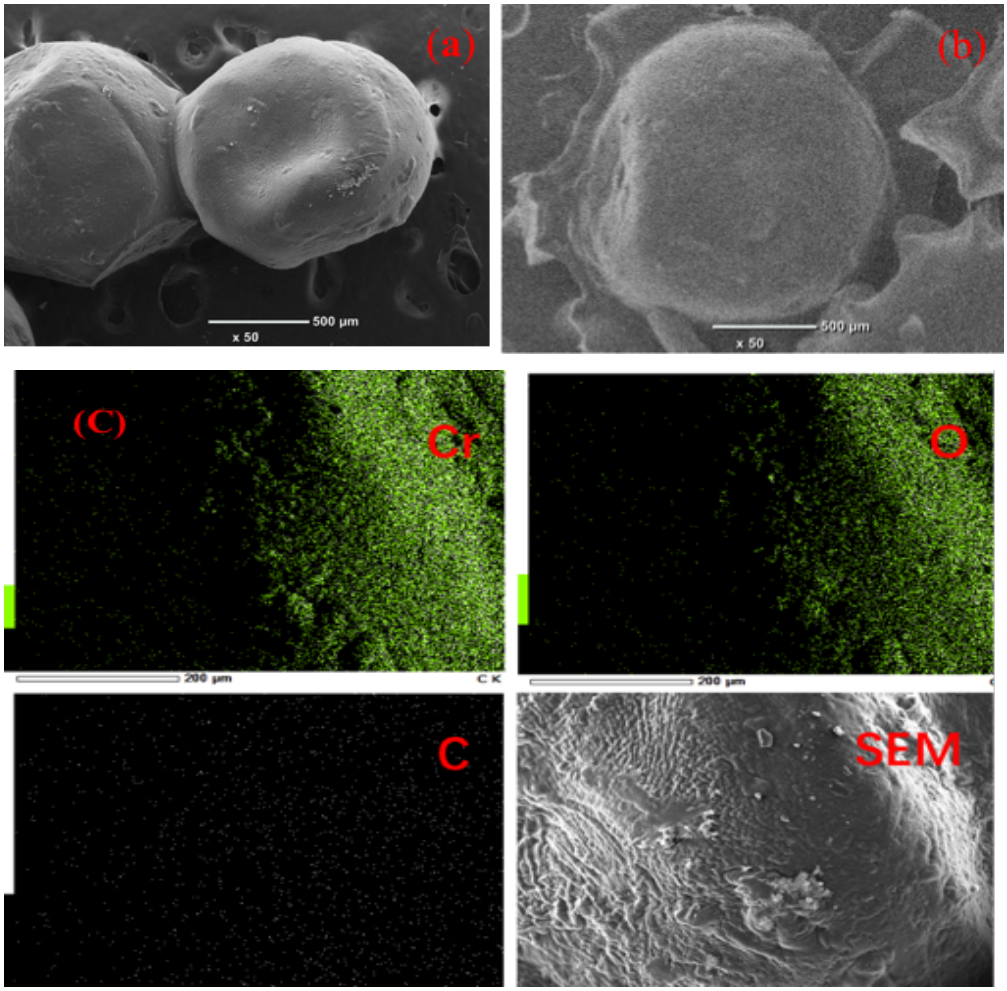

Fig. 4-1 SEM pictures of of (a) chitosan beads and (b) SDS-modified chitosan beads, and (c) mapping image of SDS-modified chitosan beads after the adsorption of Cr(VI).

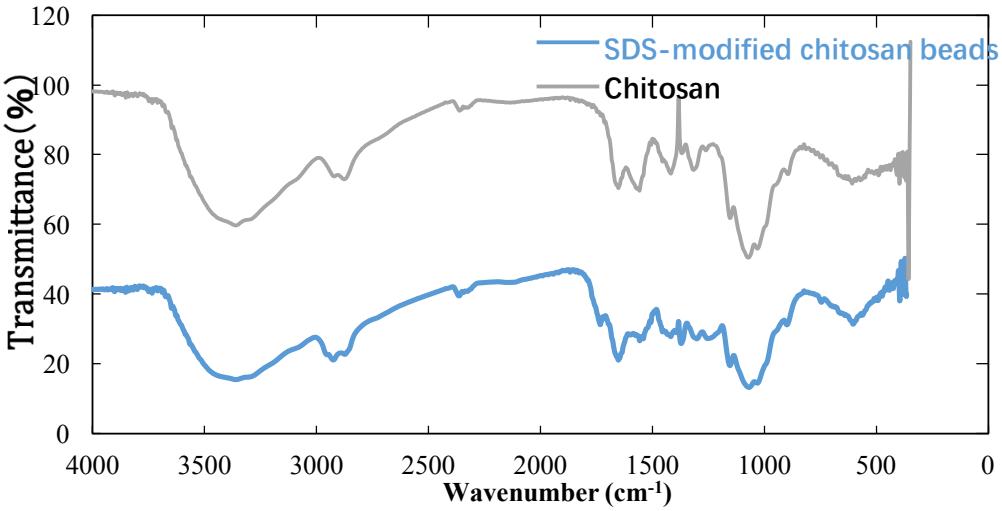

Fig. 4-2 FT-IR spectra of chitosan and SDS-modified chitosan beads

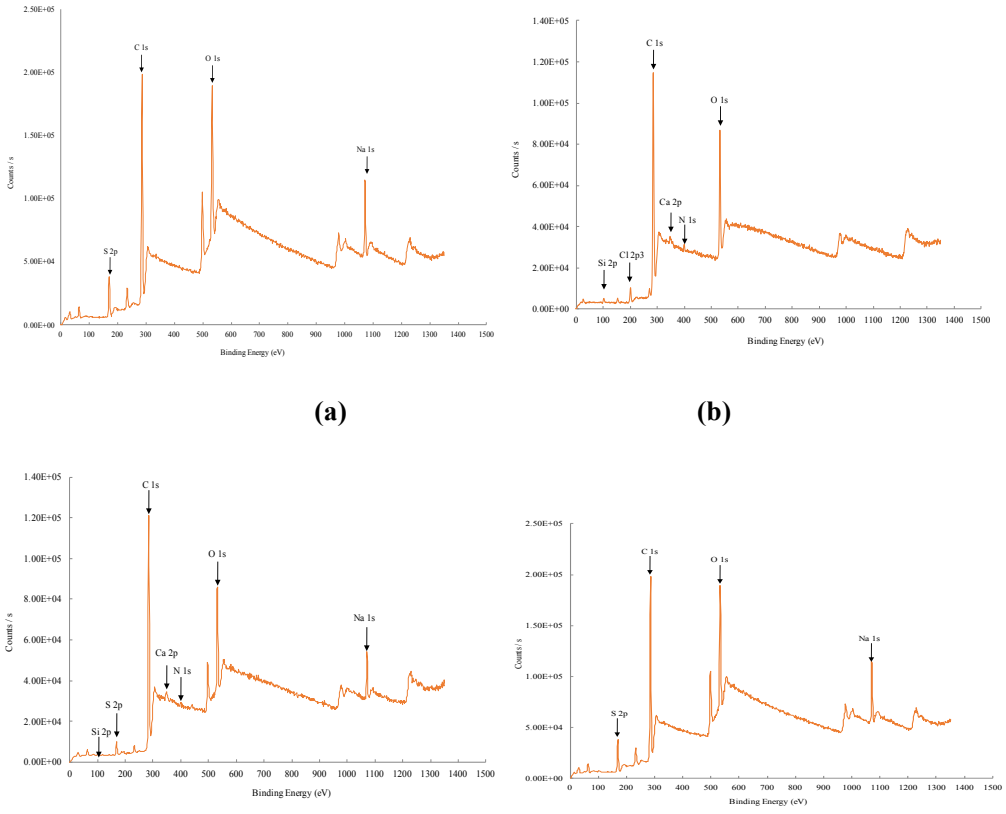

Fig. 4-3 XPS spectra of (a) chitosan, (b) SDS100-chitosan, (c) SDS600-chitosan, and (d) SDS6000-chitosan beads.

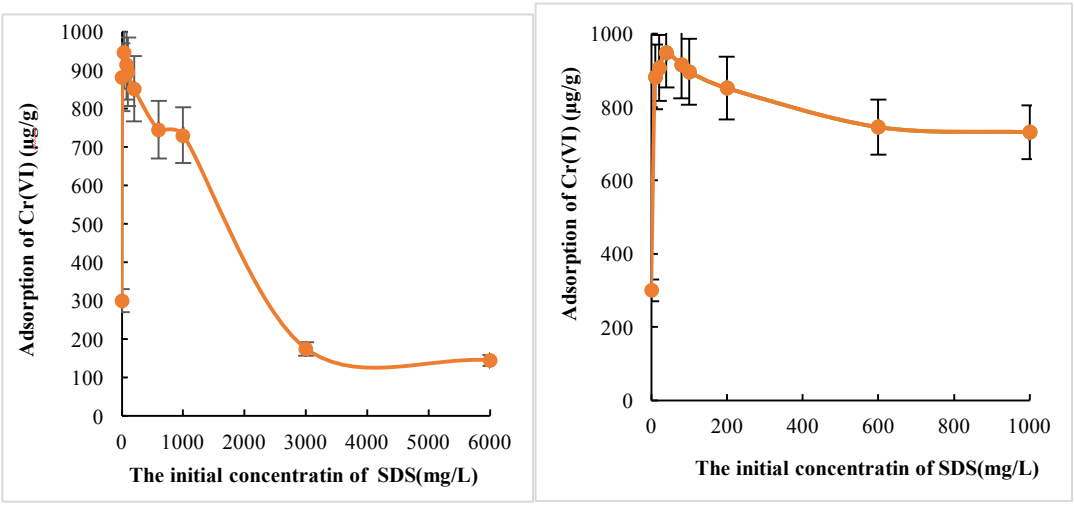

(a)Effect of initial SDS concentrations (10-6000 mg/L) on the adsorption of (Cr)(VI).
(b) Effect of initial SDS concentrations (10-1000 mg/L) on the adsorption of Cr(VI)
Fig. 4-4 Adsorption of Cr(VI) for different initial SDS concentrations (10-6000 mg/L).

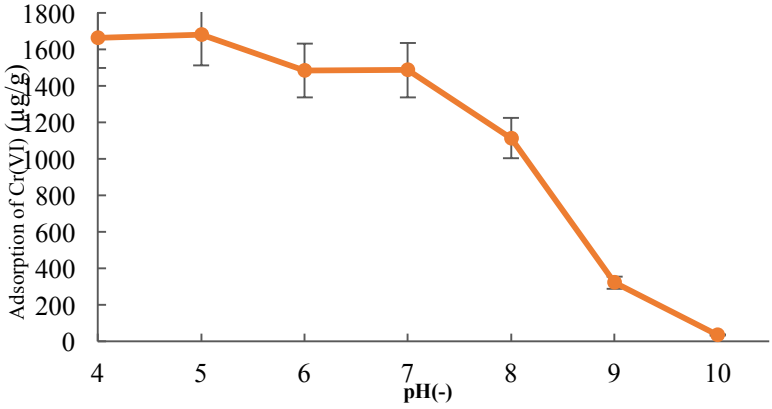

Fig. 4-5 Effect of pH on percent removal of Cr(VI) using SDS-modified chitosan beads.

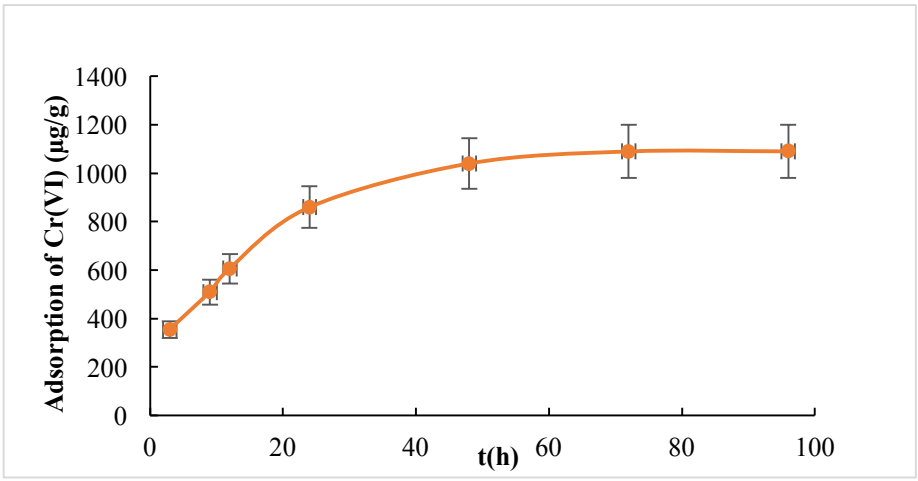

Fig. 4-6 Effect of contact time on percent removal of Cr(VI) using SDS-modified chitosan beads.

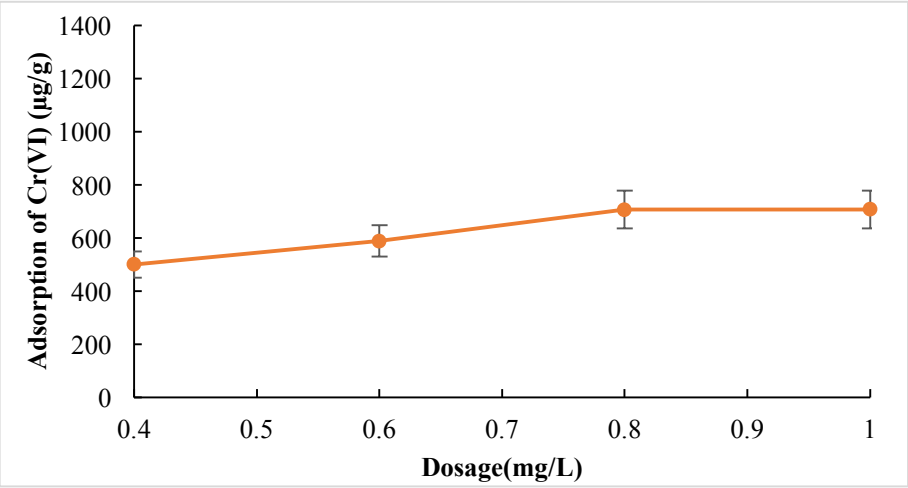

Fig. 4-7 Effect of dose on percent removal of Cr(VI) using SDS-modified chitosan beads.

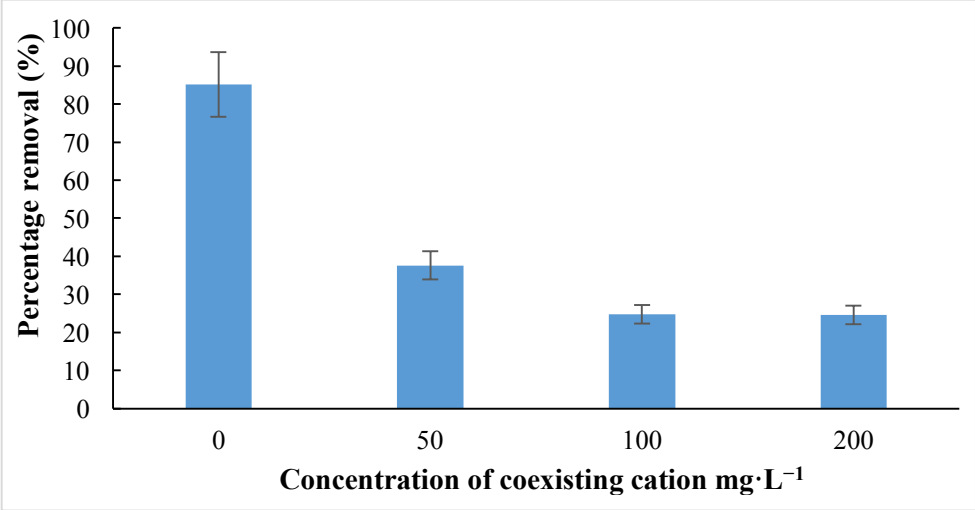

Fig. 4-8 Effect of competitive anions (Cl^-, NO_2^-, NO_3^-, and PO_4^{3-}) on the adsorption of Cr(VI) 1 mg·L^{-1} on the SDS-modified chitosan beads.

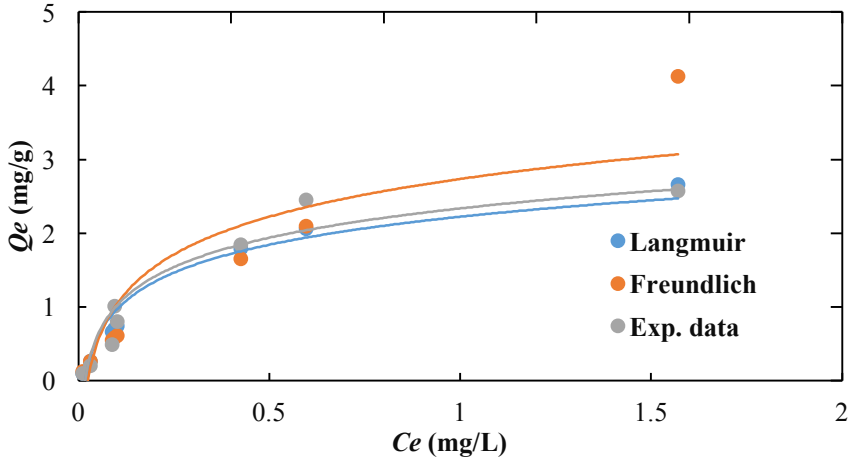

Fig. 4-9 Langmiur isotherm of Cr(VI) adsorption onto SDS-chitosan beads.

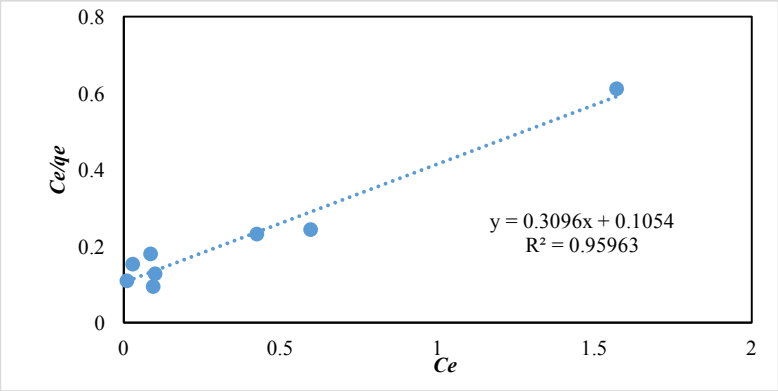

Fig. 4-10 The Langmuir isotherm of Cr(VI) adsorption on the SDS-chitosan beads.

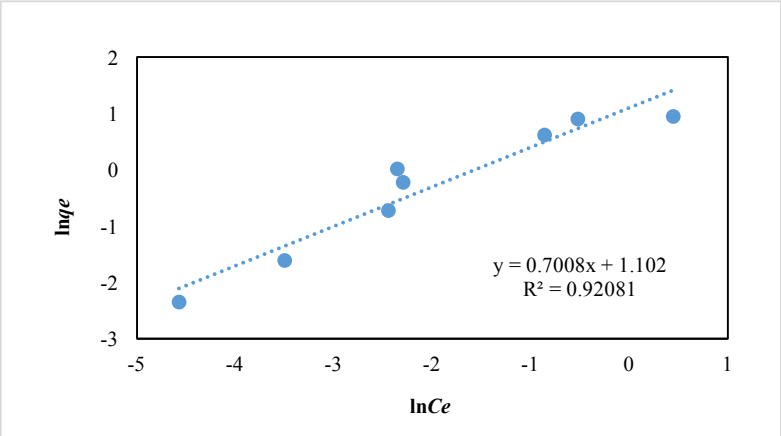

Fig. 4-11 The Freundlich isotherm of Cr(VI) adsorption on the SDS-chitosan beads.

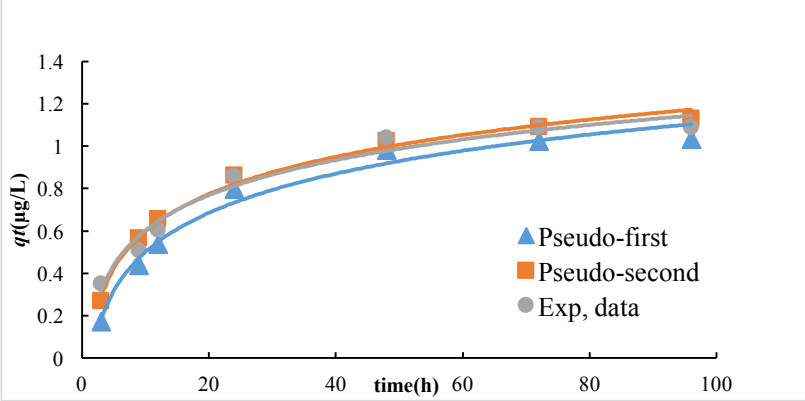

Fig. 4-12 Pseudo-first-order and pseudo-second-order plot of Cr(VI) adsorption on the SDS-chitosan beads

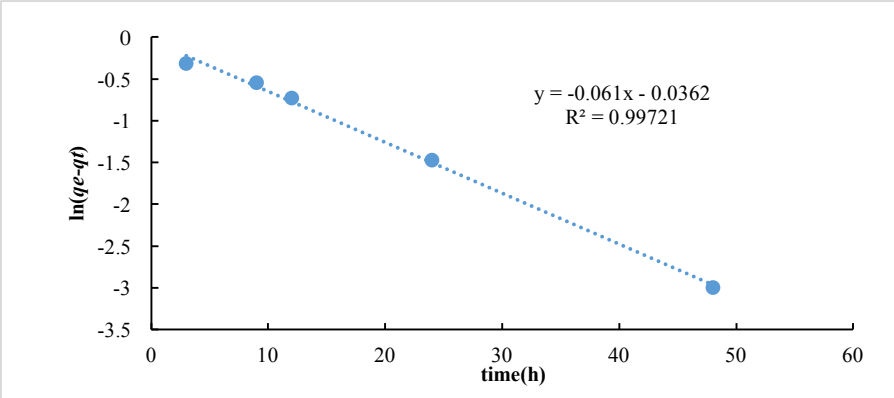

Fig. 4-13 Pseudo-first-order linear kinetic model of Cr(VI) adsorption on the SDS-chitosan beads

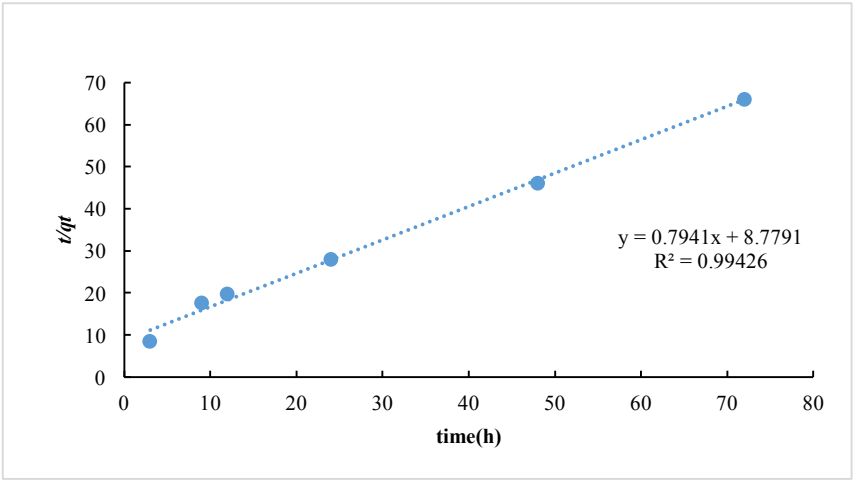

Fig. 4-14 Pseudo-secong-order linear kinetic model of Cr(VI) adsorption on the SDS-chitosan beads

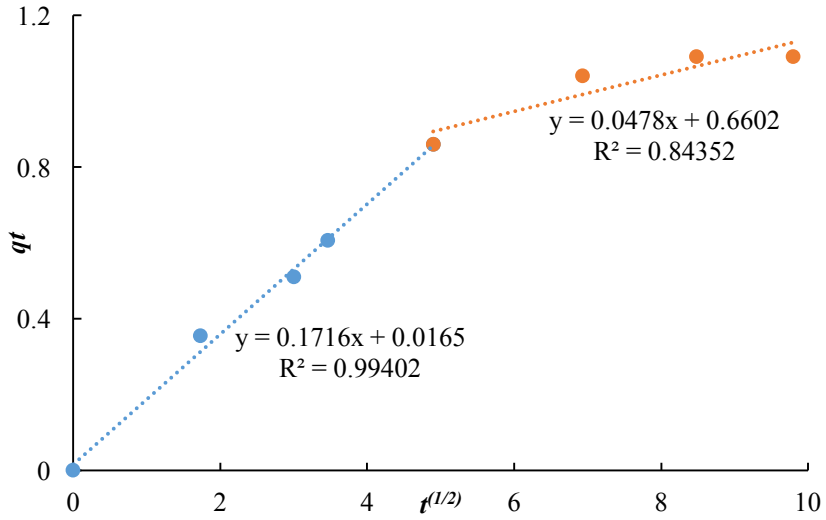

Fig. 4-15 Intraparticle plot for the adsorption of Cr(VI) by the SDS-chitosan beads

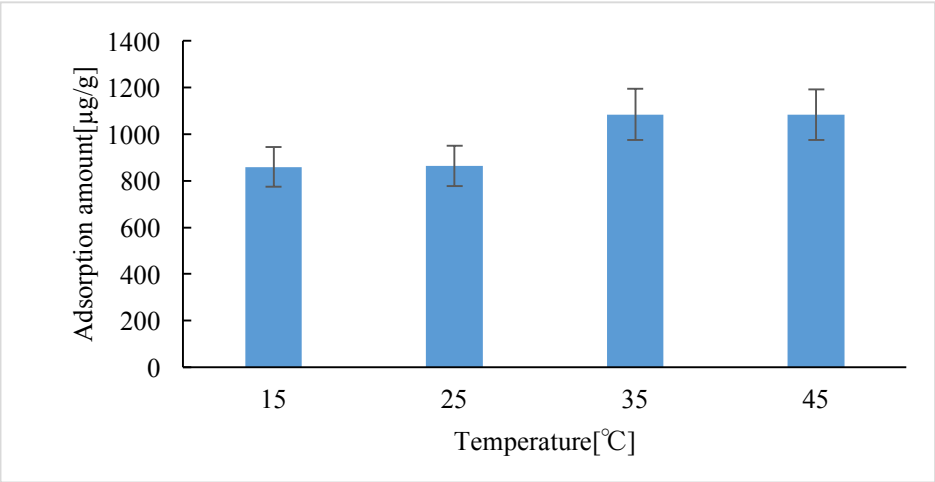

Fig. 4-16 Effect of temperature on the adsorption of Cr(VI) on the SDS-modified chitosan beads.

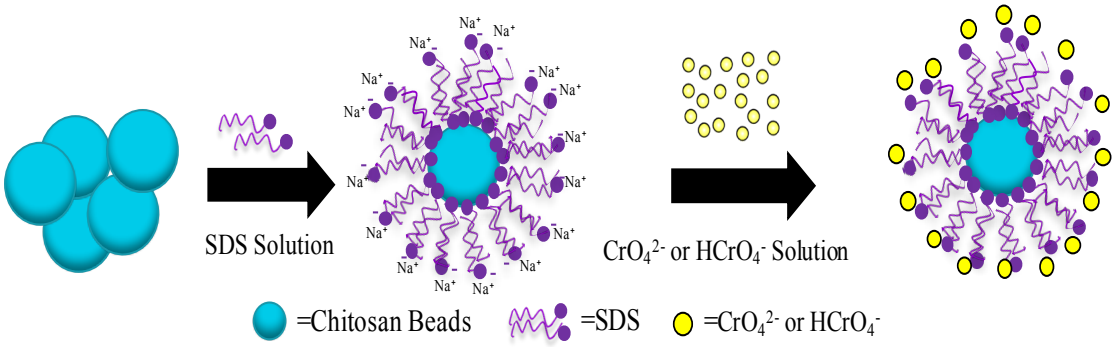

Fig. 4-17 Mechanism of Cr(VI) sorption on SDS-Chitosan Beads

Chapter 5 Conclusions

The various materials have been synthesized for removal Cr and U from aqueous solutions. The efficiency of cross-linked chitosan, SDS-chitosan beads as adsorbent for Cr and U by batch techniques were investigated. To understand the adsorption process, adsorption isotherms of Langmuir and Freundlich were investigated under the optimal conditions. In addition, the process of kinetic study is very important for understanding the reaction process and the rate of adsorption reactions. According to these studies, the following conclusions were clarified:

(1) The uptake of Cr(VI) was performed even at pH 1-3 by modified chitosan. The adsorption capacity of Cr(VI) reached maximum at pH 4 for the adsorbents.

(2) The maximum adsorption capacity of modified chitosan reached 90.9mg/g from 49.8mg/g by cross-linking with EP under our experimental conditions.

(3) The uptake of U(VI) was performed even at pH 1-3 by cross-linking. The adsorption capacity of U(VI) reached maximum at pH 5 for the adsorbents.

(4) The adsorbent (SDS-chitosan beads) showed a maximum Cr(VI) adsorption capacity of 3.23 $mg \cdot g^{-1}$ and Partition Coefficient (PC) of 9.5 $mg \cdot g^{-1} \cdot mM^{-1}$ for Cr(VI).

(5) Adsorption isotherms of Cr(VI) on the modified chitosan can be generally described by Langmuir isotherm more satisfactorily. The adsorption may have occurred mainly by monolayer reaction.

(6) The rates of adsorption using the modified chitosan for the removal of Cr(VI) and U(VI) were found to conform to pseudo-second order kinetics.

According to the above conclusions, the results show that it was quantitatively clarified to some extent that cross-linked chitosn, SDS-chitosan beads can be an

efficient adsorbent for Cr(VI) and U(VI), it is very significant information from the viewpoint of environmental protection, and can be used for treating industrial wastewaters including pollutants.

References

[1] G. Peng, G. Tian, J. Liu, Q. Bao and L. Zang, "Removal of Heavy Metals from Sewage Sludge with a Combination of Bioleaching and Electrokinetic Remediation Technology." *Desalination,* Vol. 271, pp. 100-104, 2011.

[2] S. Yesim and K. Tul, "Determination of the Biosorption Heats of Heavy Metal Ions on Zoogloea Ramigera and Rhizopus Arrhizus." *Biochemical Engineering Journal*, Vol. 6, pp. 145-151, 2000.

[3] T. M. Zewail and N. S. Yousef, "Chromium Ions (Cr^{6+} and Cr^{3+}) Removal from Synthetic Wastewater by Electrocoagulation Using Vertical Expanded Fe Anode." *Journal of Electroanalytical Chemistry*, Vol. 735, pp. 123-128, 2014.

[4] G. J. Alaerts, V. Jitjaturant and P. Kelderman, "Use of Coconut Shell Based Activated Carbon for Chromium (VI) Removal." *Water Science and Technology*, Vol. 21, pp. 1701-1704, 1989.

[5] R. S. Prakasham, J. S. Merrie, R. Sheela, N. Saswathi and S. V. Ramakrishna, "Biosorption of chromium VI by free and immobilized Rhizopus arrhizus." *Environmental pollution*, Vol. 104, pp. 421-427,1999.

[6] D. P. Mungasavalli, T. Viraraghavan and Y. C. Jin, "Biosorption of Chromium from Aqueous Solutions by Pretreated Aspergillus Niger: Batch and Column Studies." *Colloids and Surfaces, Physicochemical and, Engineering Aspects*, Vol. 301, pp. 214-223, 2007.

[7] D. Hakan, I. Demiral, T. Fatma and K. Belgin, "Adsorption of Chromium from Aqueous Solution by Activated Carbon Derived from Olive Bagasse and Applicability of Different Adsorption Models." *Chemical Engineering Journal,* Vol. 144, pp. 188-196, 2008.

[8] M. M. Rahmati, P. Rabbani, A. Abdolali, A. R. Keshtkar, "Kinetics and equilibrium studies on biosorption of cadmium, lead, and nickel ions from aqueous solutions by intact and chemically modified brown algae," *Journal of Hazardous materials,* Vol. 185, no. 1, PP. 401-407, 2011.

[9] N. Kano, K. Tanabe, M.L. Pang, Y.L. Deng and H. Imaizumi, "Biosorption of

Chromium from Aqueous Solution Using Chitosan." *J. Chem. Chem. Eng*. Vol. 8, pp. 1049-1058, 2014.

[10] G. N. Kousalya, M. R. Gandhi and S. Meenakshi, "Sorption of Chromium (VI) Using Modified Forms of Chitosan Beads." *International Journal of Biological Macromolecules*, Vol. 47, pp. 308-315, 2010.

[11] K. J. Irgolic, H. Greschonig and A． G. Howard, "Encyclopedia of Analytical Science." *New York: Academic Press*, Vol. 1, 729, 1999.

[12] O. K. Junior, L. V. A. Gurgel, R. P. Freitas, "Adsorption of Cu(II), Cd(II), and Pb(II) from aqueous single metal solutions by mercerized cellulose and mercerized sugarcane bagasse chemically modified with EDTA dianhydride." *Carbohydrate Polymers*, Vol. 77, no. 3. pp. 643-650, 2009.

[13] L. Pietrelli, I. Francolini, A. Piozzi, M. Sighicelli, I. Silvestro, M. Vocciante, "Chromium (III) Removal from Wastewater by Chitosan Flakes." *Appl. Sci.*, Vol. 10, pp. 1925, 2020.

[14] L. Pietrelli, N. M. Ippolito, A. P. Reverberi, M. Vocciante, "Heavy Metals Removal and Recovery from Hazardous Leather Sludge." *Chem. Eng. Trans.*, Vol. 76, pp. 1327-1332, 2019.

[15] A. U. Rajapaksha, M. S. Alam,; N. Chen, D. S. Alessi, A. D. Igalavithana, D. C. W. Tsang, Y. S. Ok, "Removal of hexavalent chromium in aqueous solutions using biochar: Chemical and spectroscopic investigations." *Sci. Total Environ.*, Vol. 625, pp. 1567-1573, 2018.

[16] S. Shi, J. Yang, S. Liang, M. Li, Q. Gan, K. Xiao, J. P. Hu, "Enhanced Cr (VI) removal from acidic solutions using biochar modified by Fe_3O_4@SiO_2-NH_2 particles." *Sci. Total Environ.*, Vol. 628, pp. 499-508, 2018.

[17] Y. Wang, N. Zhang, D. Chen, D. Ma, G. Liu, X. Zou, Y. Chen, R. Shu, Q. Song, W. Lv, "Facile synthesis of acid- modified UiO-66 to enhance the removal of Cr (VI) from aqueous solutions." *Sci. Total Environ.,* Vol. 682, pp. 118-127, 2019.

[18] N. Sankararamakrishnan, A. Dixit, L. Iyengar, R. Sanghi, "Removal of hexavalent chromium using a novel cross linked xanthated chitosan," *Bioresource Technology*, Vol. 97, no. 18, pp. 2377-2382, 2006.

[19] K. Harmsen, F.A.M. De Haan, "Occurrence and Behaviour of Uranium and Thorium in Soil and Water." *Neth. J. Agric. Sci.*, Vol. 28, pp. 40-62, 1980.

[20] L. Duquène, F. Tack, E. Meers, J. Baeten, J. Wannijn, H. Vandenhove, "Effect of Biodegradable Amendments on Uranium Solubility in Contaminated Soils." *Sci. Total Environ.* Vol. 391, pp. 26-33, 2008.

[21] B. Chen, P. Roos, Y.G. Zhu, I. Jakobsen, "Arbuscular Mycorrhizas Contribute to Phytostabilization of Uranium in Uranium Mining Tailings." *J. Environ. Radioact.* Vol. 99, pp. 801-810, 2008.

[22] M.M.S.C. Pinto, M.M.V.G. Silva, A.M.R. Neiva, "Pollution of Water and Stream Sediments Associated with the Vale de Abrutiga Uranium Mine, Central Portugal." *Mine Water Environ.* Vol. 23, pp. 66-75, 2004.

[23] M.M.S.C. Pinto, M.M.V. Silva, A.M.R. Neiva, F. Guimarães, P.B. Silva, "Release, Migration, Sorption, and (Re) Precipitation of U during Peraluminous Granite Alteration under Oxidizing Conditions in Central Portugal." *Geosciences.* Vol. 8, pp. 95, 2018.

[24] M. Pinto, M.S. Cabral, M.M. Silva, "The Vale de Abrutiga Uranium Phosphates mine, Central Portugal." *Chem. Erde.* Vol. 67, pp. 251-252, 2007.

[25] C. Pinto, M.S. Marina, M.V.G. Silva, A.M.R. Neiva, "Geochemistry of U-bearing Minerals at Vale de Abrutiga Uranium Mine, Central Portugal." *Neues Jahrb. Mineral. Abh.* Vol. 185, pp. 183-198, 2008.

[26] Z. Fischerová, P. Tlustoš, J. Száková, K. A. Šichorova, "Comparison of Phytoremediation Capability of Selected Plant Species for Given Trace Elements." *Environ. Pollut.* Vol. 144, pp. 93-100, 2006.

[27] B. Allard, U. Olofsson, B, Torstenfelt, "Environmental actinide chemistry." *Inorg. Chim. Actaf.* Vol. 94, pp. 205-221, 1984.

[28] J. Kotas, Z. Stasicka, "Chromium occurrence in the environment and methods of its speciation." *Environmental Pollution*, Vol. 107, pp. 263-283, 2000.

[29] Y. A. Aydın, N.D. Aksoy, "Adsorption of chromium on chitosan: optimization, kinetics and thermodynamic." *J. Chem. Eng.* Vol. 151, pp. 188-194, 2009.

[30] X.Y. Li, H.H. Zhou, W.Q. Wu, S.D. Wei, Y. Xu, Y.F. Kuang. "Studies of heavy metal ion on chitosan/sulfydryl-functionalized graphene oxide composites." *J. Colloid. Interf. Sci.* Vol. 448, pp. 389-397, 2015.

[31] D. Kołod´ nska., “Chitosan as an effective low-cost sorbent of heavy metal complexes with the polyaspartic acid.” *J. Chem. Eng.* Vol. 173, pp. 520-529, 2011.

[32] Z. Modrzejewska, W. Sujka, M. Dorabialska, R. Zarzycki, “Adsorption of Cr(VI) on Cross-linked Chitosan Beads.” *Sci. Technol.* Vol. 41, pp. 111-122, 2006.

[33] K. Jaros, W. Kaminski, J. Albinska, U. Nowak, “Removal of Heavy Metal Ions: Copper, Zinc and Chromium from Water on Chitosan Beads.” *Environ. Prot. Eng.* Vol. 31, pp. 153-162, 2005.

[34] R. Zarzycki, W. Sujka, M. Dorabialska, Z. Modrzejewska, “Adsorption of Cr(VI) on Chitosan Beads.” *Chem. Inz. Ekol.* Vol. 9, pp. 1561-1570, 2002.

[35] W. S. Ngah, C. S. Endud, R. Mayanar, “Removal of Copper (II) Ions from Aqueous Solution onto Chitosan and Cross-linked Chitosan Beads.” *React. Funct. Polym.* Vol. 50, pp. 181-190, 2002.

[36] Cestari, A. R., Vieira, E. F. S., Oliveira, I. A., Bruns, R. E. “The removal of Cu (II) and Co (II) from aqueous solutions using cross-linked chitosan-evaluation by the Factorial Design Methodology.” *J. Hazard. Mater.* Vol. 143, pp. 8-16, 2007.

[37] G. Wang, J. Liu, X. Wang, Z.Y. Xie, N. Deng, “Adsorption of Uranium(VI) from Aqueous Solution onto Cross-Linked Chitosan.” *J. Hazard Mater.* Vol. 168, pp. 1053-1058, 2009.

[38] E. Guibal, A. Larkin, T. Vincent, J.M. Tobin, “Chitosan sorbents for platinum sorption from dilute solutions.” *Ind. Eng. Chem. Res.*, Vol. 38, no. 10, pp. 4011-4022, 1999.

[39] J. Guzman, I. Saucedo, J. Revilla, R. Navarro, E. Guibal, “Vanadium interactions with chitosan: influence of polymer protonation and metal speciation.” *Langmuir.* Vol. 18, no. 5, pp. 1567-1573, 2002.

[40] C. Gerente, V. C. Lee, P. L. Cloirec, G. McKay, “Application of Chitosan for the Removal of Metals from Wastewaters by Adsorption-Mechanisms and Models Review. Critical Reviews in Environmental Science and Technology.” Vol. 37, pp. 41-127, 2007.

[41] E. Repoa, J.K. Warchoł, A. Bhatnagar, M. Sillanpää, “Heavy metals adsorption by novel EDTA-modified chitosan–silica hybrid materials.” *J. Colloid Interface Sci.* Vol. 358, no. 2, pp. 261-267, 2011.

[42] A.J. Varma, S.V. Deshpande, J.F. Kennedy, “Metal complexation by chitosan and its derivatives: a review.” *Carbohydr. Polym*. Vol. 55, no. 1, pp. 77-93, 2004.

[43] P.K. Dutta, J. Dutta, M.C. Chattopadhyaya, V.S. Tripathi, “Chitin and chitosan: novel biomaterials waiting for future developments.” *J. Polym. Mater.* Vol. 21, pp. 321-333, 2004.

[44] G. Kyzas, D. Bikiaris, “Recent modifications of chitosan for adsorption applications: a critical and systematic review.” *Mar. Drugs.* Vol. 13, pp. 312-337, 2015.

[45] B. Bolto, J. Gregory, “Organic polyelectrolytes in water treatment.” *Water Res.* Vol. 41, no. 11, pp. 2301-2324, 2007.

[46] J. Gregory, S. Barany, “Adsorption and flocculation by polymers and polymer mixtures.” *Adv. Colloid Interface Sci.* Vol. 169, no. 1, pp. 1-12, 2011.

[47] M.S. Nasser, A.E. James, “The effect of polyacrylamide charge density and molecular weight on the flocculation and sedimentation behaviour of kaolinite suspensions.” *Sep. Purif. Technol.* Vol. 52, no. 2, pp. 241-252, 2006.

[48] L. Mathieu, B. Benoit, “Understanding the roles and characterizing the intrinsic properties of synthetic vs. natural polymers to improve clarification through interparticle Bridging: A review.” *Sep. Purif. Technol.*, Vol. 231, pp. 115893-115917, 2020.

[49] D. Das.; A. Pal. “Adsolubilization phenomenon perceived in chitosan beads leading to a fast and enhanced malachite green removal.” *J. Chem. Eng.*, Vol. 290, pp. 371-380, 2016.

[50] Y. Wu, H.J. Luo, H. Wang, C. Wang, J. Zhang, Z.L. Zhang, “Adsorption of Hexavalent Chromium from Aqueous Solutions by Graphene Modified with Cetyltrimethylammonium Bromide.” *J. Colloid Interface Sci.*, Vol. 394, pp. 183-191, 2013.

[51] M. H. Sui, Y. F. Zhou, L. Sheng B. B. Duan, “Adsorption of Norfloxacin in Aqueous Solution by Mg-Al Layered Double Hydroxides with Variable Metal Composition and Interlayer Anions”, *Chemical Engineering Journal*, Vol. 210, pp. 451-660, 2012.

[52] X. F. Liang, W. G. Hou, Y. M. Xu, et al. “Sorption of Lead Ion by Layered Double Hydroxide Intercalated with Diethylenetriaminepentaacetic Acid”, *Colloids and Surfaces A: Physicochemical and Engineering Aspects*, Vol. 366, no. 1, pp. 50-57, 2010.

[53] C.J. Na, M.J. Yoo, D.C.W. Tsang, H.W. Kim, K.H. Kim, “High-performance materials for effective sorptive removal of formaldehyde in air.” *J. Hazard. Mater.,* Vol. 366, pp. 452-465, 2019.

[54] S. Zhang, N. Kano, K. Mishima, H. Okawa, “Adsorption and Desorption Mechanisms of Rare Earth Elements (REEs) by Layered Double Hydroxide (LDH) Modified with Chelating Agents.” *Appl. Sci.* Vol. 9, pp. 4805, 16 pages, 2019.

[55] S.W. Won, S. B. Choi, Y.S. Yun “Performance and mechanism in binding of Reactive Orange 16 to various types of sludge,” *Biochem Eng J.*, Vol. 28, pp. 208-214, 2006.

[56] B. Wang, Guo Xianghai, B. Peng, “Removal technology of boron dissolved in aqueous solutions-A review.” *Colloids and Surfaces A: Physicochemical and Engineering Aspects*, Vol. 444, pp. 338-344, 2014.

[57] D. L. Zhao, G. D. Sheng, J. Hu, C. L. Chen, X. K. Wang, “The adsorption of Pb(II) on Mg_2Al layered double hydroxide”, *Chemical Engineering Journal*, Vol. 171, pp. 167-174, 2011.

[58] N. Ayawei, C. Y. Abasi, D. Wankasi, E. D. Dikio, “Layered Double Hydroxide Adsorption of Lead: Equilibrium, Thermodynamic and Kinetic Studies.” *International Journal of Advanced Research in Chemical Science (IJARCS),* Vol. 2, no. 5, pp. May 22-32, 2015.

[59] N. Ayawei, A. T. Ekubo, D. Wankasi, E. D. Dikio, “Synthesis and Application of Layered Double Hydroxide for the removal of Copper in Wastewater”, *International Journal of Chemistry*, Vol. 7, no. 1, pp. 122-132, 2015.

[60] N. Ayawei, A. T. Ekubo, D. Wankasi, E. D. Dikio, "Adsorption Dynamics of Copper Adsorption by Zn/Al-CO_3". *IJACSA.* Vol. 3, no. 1, pp. 57-64, 2015.

[61] R. N. Aleksandra, J. V. Sava, G. A. Dusan, "Modification of chitosan by zeolite A and adsorption of Bezactive Orange 16 from aqueous solution", *Composites: Part B*, Vol. 53, pp. 145-151, 2013.

[62] L. Dolatyari, M. R. Yaftian, S. Rostamnia, "Adsorption characteristics of Eu(III) and Th(IV) ions onto modified mesoporous silica SBA-15 materials." *Journal of the Taiwan Institute of Chemical Engineers*, Vol. 60, pp. 174-184, 2016.

[63] B. KUTCHKO, A. KIM, "Fly ash characterization by SEM–EDS." *Fuel*., Vol. 85, no. 17-18, pp. 2537-2544, 2006.

[64] D. E. Newbury, N. W. M. Ritchie, "Is Scanning Electron Microscopy/Energy Dispersive X-ray Spectrometry (SEM/EDS) Quantitative?" *Scanning*, Vol. 35, no. 3, pp. 141-168, 2012.

[65] S. R. Kelemen, G. N. George, M. L. Gorbaty, (1990). "Direct determination and quantification of sulphur forms in heavy petroleum and coals." *Fuel*, Vol. 69, no. 8, pp. 939-944, 1990.

[66] M. Chen, X. Wang, Y. Yu, Z. Pei, et al. "X-ray photoelectron spectroscopy and auger electron spectroscopy studies of Al-doped ZnO films." *Applied Surface Science,* Vol. 158, no. 1-2, pp. 134-140, 2000.

[67] Y. Chen, C. Zou, M. Mastalerz, S. Hu, C. Gasaway, X. Tao, "Applications of Micro-Fourier Transform Infrared Spectroscopy (FTIR) in the Geological Sciences-A Review." *International Journal of Molecular Sciences*, Vol. 16, no. 12, pp. 30223-30250, 2015.

[68] Z. Movasaghi, S. Rehman, D. I. ur Rehman, "Fourier Transform Infrared (FTIR) Spectroscopy of Biological Tissues." *Applied Spectroscopy Reviews*, Vol. 43, no. 2, pp. 134-179, 2008.

[69] S.J. Seaman, M.D. Dyar, N. Marinkovic, N.W. Dunbar, "An FTIR study of hydrogen in anorthoclase and associated melt inclusions." *American Mineralogist*, Vol. 91, pp. 12-20, 2006.

[70] J. H. Dane, C. G. Topp, K. D. Pennell, "2.5 Specific Surface Area." *SSSA Book Series.* 2002.

[71] S. Kaufhold, R. Dohrmann, M. Klinkenberg, S. Siegesmund, K. Ufer, "N_2-BET specific surface area of bentonites." *Journal of Colloid and Interface Science*, Vol. 349, no. 1, pp. 275-282, 2010.

[72] R. Lobinski, D. Schaumloffel, J. Szpunar, "Mass spectrometry in bioinorganic analytical chemistry." *Mass Spectrom. Rev.* Vol. 25, pp. 255, 2006.

[73] A.L. Rosen, G.M. Hieftje, "Inductively coupled plasma mass spectrometry and electrospray mass spectrometry for speciation analysis: applications and instrumentation." *Spectrochim. Acta, Part B-Atomic Spectrosc.* Vol. 59, pp. 135, 2004.

[74] Adrian A. Ammann, "Inductively coupled plasma mass spectrometry (ICP MS): a versatile tool." *J. Mass Spectrom.*, Vol. 42, pp. 419-427, 2007.

[75] G.Peng, G. Tian, J. Liu, Q. Bao and L. Zang, "Removal of Heavy Metals from Sewage Sludge with a Combination of Bioleaching and Electrokinetic Remediation Technology." *Desalination*, Vol. 271, pp. 100-104, 2011.

[76] S. Yesim and K. Tul, "Determination of the Biosorption Heats of Heavy Metal Ions on Zoogloea Ramigera and Rhizopus Arrhizus." Biochemical Engineering Journal, Vol. 6, pp. 145-151, 2000.

[77] T. M. Zewail and N. S. Yousef, "Chromium Ions (Cr6+ and Cr3+) Removal from Synthetic Wastewater by Electrocoagulation Using Vertical Expanded Fe Anode." Journal of Electroanalytical Chemistry, Vol. 735, pp. 123-128, 2014.

[78] G. J. Alaerts, V. Jitjaturant and P. Kelderman, "Use of Coconut Shell Based Activated Carbon for Chromium (VI) Removal." Water Science and Technology, Vol. 21, pp. 1701-1704, 1989.

[79] R. S. Prakasham, J. S. Merrie, R. Sheela, N. Saswathi and S. V. Ramakrishna, "Biosorption of chromium VI by free and immobilized Rhizopus arrhizus." *Environmental pollution*, Vol. 104, pp. 421-427,1999.

[80] D. P. Mungasavalli, T. Viraraghavan and Y. C. Jin, "Biosorption of Chromium from Aqueous Solutions by Pretreated Aspergillus Niger: Batch and Column

Studies." Colloids and Surfaces, Physicochemical and, Engineering Aspects, Vol. 301, pp. 214-223, 2007.

[81] D. Hakan, I. Demiral, T. Fatma and K. Belgin, "Adsorption of Chromium from Aqueous Solution by Activated Carbon Derived from Olive Bagasse and Applicability of Different Adsorption Models." Chemical Engineering Journal, Vol. 144, pp. 188-196, 2008.

[82] M. M. Rahmati, P. Rabbani, A. Abdolali, A. R. Keshtkar, "Kinetics and equilibrium studies on biosorption of cadmium, lead, and nickel ions from aqueous solutions by intact and chemically modified brown algae," Journal of Hazardous materials, Vol. 185, no. 1, PP. 401-407, 2011.

[83] A. M. Motawie, K. F. Mahmoud, A. A. El-Sawy, et al. "Preparation of chitosan from the shrimp shells and its application for pre-concentration of uranium after cross-linking with epichlorohydrin." *J. Egyptian Journal of Petroleum.* Vol. 23, no. 2, PP. 221-228, 2014.

[84] W. S. Ngah, C. S. Endud, R. Mayanar, "Removal of Copper (II) Ions from Aqueous Solution onto Chitosan and Cross-linked Chitosan Beads." *React. Funct. Polym.* Vol. 50, PP. 181-190, 2002.

[85] A. R. Cestari, E. F. S. Vieira, I. A. Oliveira, R. E. Bruns, "The removal of Cu (II) and Co (II) from aqueous solutions using cross-linked chitosan-evaluation by the Factorial Design Methodology." *J. Hazard. Mater.* Vol. 143, PP. 8-16, 2007.

[86] Y.J. Zhang, J.H. Lan, L. Wang, Q.Y. Wu, C.Z. Bo, T. Wang, Z.F. Chai, W.Q. Shi, "Adsorption of Uranyl Species on Hydroxylated Titanium Carbide Nanosheet: A First-Principle Study." *J. Hazard. Mater.* Vol. 308, pp. 402-410, 2016.

[87] C.K.D. Hsi, "Langmuir, D. Adsorption of Uranyl onto Ferric Oxyhydroxides: Application of the Surface Complexation Site-binding Model." *Geochim. Cosmochim. Acta*. Vol. 49, pp. 1931-1941, 1985.

[88] I.A. Katsoyiannis, "Carbonate Effects and pH-dependence of Uranium Sorption onto Bacteriogenic Iron Oxides: Kinetic and Equilibrium Studies." *J. Hazard. Mater.* Vol. 139, pp. 31-37, 2007.

[89] C. Gerente, V.C. Lee, P.L. Cloirec, G. McKay, “Application of Chitosan for the Removal of Metals from Wastewaters by Adsorption-Mechanisms and Models Review.” *Crit. Rev. Environ. Sci. Technol.*, Vol. 37, pp. 41-127, 2007.

[90] E. Repoa, J.K. Warchoł, A. Bhatnagar, M. Sillanpää, “Heavy metals adsorption by novel EDTA-modified chitosan-silica hybrid materials.,” *J. Colloid Interface Sci.*, Vol. 358, pp. 261-267, 2011.

[91] A.J. Varma, S.V. Deshpande, J.F. Kennedy, “Metal complexation by chitosan and its derivatives: A review.” *Carbohydr. Polym.*, Vol, 55. pp. 77-93, 2004.

[92] P.K. Dutta, J. Dutta, M.C. Chattopadhyaya, V.S. Tripathi, “Chitin and chitosan: Novel biomaterials waiting for future developments.” *J. Polym. Mater.*, Vol. 21. pp. 321-333, 2004.

[93] G.Z. Kyzas, D.N. Bikiaris, “Recent modifications of chitosan for adsorption applications: A critical and systematic review.” *Mar. Drugs.*, Vol. 13, pp. 312-337, 2015.

[94] B. Bolto, J. Gregory, “Organic polyelectrolytes in water treatment.” *Water Res.*, Vol. 41, pp. 2301-2324, 2007.

[95] J. Gregory, S. Barany, “Adsorption and flocculation by polymers and polymer mixtures.” *Adv. Colloid Interface Sci.*, Vol. 169, pp. 1-12, 2011.

[96] M.S. Nasser, A.E. James, “The effect of polyacrylamide charge density and molecular weight on the flocculation and sedimentation behaviour of kaolinite suspensions.” *Sep. Purif. Technol*., Vol. 52, pp. 241-252, 2006.

[97] L. Mathieu, B. Benoit, “Understanding the roles and characterizing the intrinsic properties of synthetic vs. natural polymers to improve clarification through interparticle Bridging: A review.” *Sep. Purif. Technol.*, Vol. 231, pp. 115893-115917, 2020.

[98] P. Pal, A. Pal, “Surfactant-modified chitosan beads for cadmium ion adsorption.” *Int. J. Biol. Macromol.*, Vol. 104, pp. 1548–1555, 2017.

[99] P. Pal, A. Pal, “Treatment of real wastewater: Kinetic and thermodynamic aspects of cadmium adsorption onto surfactant-modified chitosan beads.” *Int. J. Biol. Macromol.* Vol. 131, pp. 1092-1100, 2019.

[100] G. Peng, G. Tian, J. Liu, Q. Bao and L. Zang, “Removal of Heavy Metals from Sewage Sludge with a Combination of Bioleaching and Electrokinetic Remediation Technology.” Desalination, Vol. 271, pp. 100-104, 2011.

[101] S. Yesim and K. Tul, “Determination of the Biosorption Heats of Heavy Metal Ions on Zoogloea Ramigera and Rhizopus Arrhizus.” Biochemical Engineering Journal, Vol. 6, pp. 145-151, 2000.

[102] T. M. Zewail and N. S. Yousef, “Chromium Ions (Cr6+ and Cr3+) Removal from Synthetic Wastewater by Electrocoagulation Using Vertical Expanded Fe Anode.” Journal of Electroanalytical Chemistry, Vol. 735, pp. 123-128, 2014.

[103] G. J. Alaerts, V. Jitjaturant and P. Kelderman, “Use of Coconut Shell Based Activated Carbon for Chromium (VI) Removal.” Water Science and Technology, Vol. 21, pp. 1701-1704, 1989.

[104] R. S. Prakasham, J. S. Merrie, R. Sheela, N. Saswathi and S. V. Ramakrishna, “Biosorption of chromium VI by free and immobilized Rhizopus arrhizus.” *Environmental pollution*, Vol. 104, pp. 421-427,1999.

[105] D. P. Mungasavalli, T. Viraraghavan and Y. C. Jin, “Biosorption of Chromium from Aqueous Solutions by Pretreated Aspergillus Niger: Batch and Column Studies.” Colloids and Surfaces, Physicochemical and, Engineering Aspects, Vol. 301, pp. 214-223, 2007.

[106] D. Hakan, I. Demiral, T. Fatma and K. Belgin, “Adsorption of Chromium from Aqueous Solution by Activated Carbon Derived from Olive Bagasse and Applicability of Different Adsorption Models.” Chemical Engineering Journal, Vol. 144, pp. 188-196, 2008.

[107] M. M. Rahmati, P. Rabbani, A. Abdolali, A. R. Keshtkar, “Kinetics and equilibrium studies on biosorption of cadmium, lead, and nickel ions from aqueous solutions by intact and chemically modified brown algae,” Journal of Hazardous materials, Vol. 185, no. 1, PP. 401-407, 2011.

[108] A. M. Motawie, K. F. Mahmoud, A. A. El-Sawy, et al. “Preparation of chitosan from the shrimp shells and its application for pre-concentration of uranium after

cross-linking with epichlorohydrin." *J. Egyptian Journal of Petroleum.* Vol. 23, no. 2, PP. 221-228, 2014.

[109] W. S. Ngah, C. S. Endud, R. Mayanar, "Removal of Copper (II) Ions from Aqueous Solution onto Chitosan and Cross-linked Chitosan Beads." *React. Funct. Polym.* Vol. 50, PP. 181-190, 2002.

[110] A. R. Cestari, E. F. S. Vieira, I. A. Oliveira, R. E. Bruns, "The removal of Cu (II) and Co (II) from aqueous solutions using cross-linked chitosan-evaluation by the Factorial Design Methodology." *J. Hazard. Mater.* Vol. 143, PP. 8-16, 2007.

[111] Lazaridis, N.K.; Asouhidou, D.D. Kinetics of sorptive removal of chromium(VI) from aqueous solutions by calcined Mg-Al-CO3 hydrotalcite. *Water Res.* 2003, 37, 2875-2882.

[112] Ho, Y.S.; Mckay, G. The sorption of lead(II) ions on peat. *Water Res.* 1999, 33, 578-584.

[113] Weber, W.J.; Morris, J.C. Kinetics of adsorption on carbon from solution. *Asce Sanitary Eng. Div. J.* 1963, 1, 1-2.

[114] Yan, L.G.; Yang, K.; Shan, R.R.; Yan, T.; Wei, J.; Yu, S.H.; Yu, H.Q.; Du, B. Kinetic isotherm and thermodynamic investigations of phosphate adsorption onto core-shell Fe3O4@LDHs composites with easy magnetic separation assistance. *J. Colloid Interf. Sci.* 2015, 448, 508-516.

[115] Jaycock, M.J.; Parfitt, G.D. Chemistry of Interfaces. Ellis Horwood Chichester. 1981.

[116] Nithya, R.; Thandapani, Gomathi.; Sudha, P. N.; Jayachandran, Venkatesan.; Sukumaran, Anil.; SeKwon, Kim. Removal of Cr(VI) from aqueous solution using chitosan-g-poly (butyl acrylate)/silica gel nanocomposite. *Int. J. Biol. Macromol.* 2016, 7, 545-554.

[117] Liu, Q.; B. Yang, Zhang, L.; Huang, R. Adsorptive removal of Cr(VI) from aqueous solutions by cross-linked chitosan/bentonite composite. Korean *J. Chem. Eng*. 2015, 32 (7), 1314-1322.

[118] Zhang, L.; Luo, H.; Liu, P.; Fang, W.; Geng, J. Anovelmodified graphene oxide/chitosan composite used as an adsorbent for Cr(VI) in aqueous solutions. *Int. J. Biol. Macromol.* 2016, 87, 586-596.

[119] Hu, X.J.; Wang, J.S.; Liu, Y.G.; Li, X.; Zeng, G.M.; Bao, Z.L.; Zeng, X.X.; Chen, A.W.; Long, F. Adsorption of chromium (VI) by ethylenediamine-modified cross-linked magnetic chitosan resin: isotherms, kinetics and thermodynamics. *J. Hazard. Mater.* 2011, 185 (1), 306-314.

[120] Xiao, L.; Ma, W.; Han, M.; Cheng, Z. The influence of ferric iron in calcined nano-Mg/Al hydrotalcite on adsorption of Cr (VI) from aqueous solution. *J. Hazard. Mater.* 2011, 186, 690-698.

[121] L. Zhang, H. Luo, P. Liu, W. Fang, J. Geng, Anovelmodified graphene oxide/chitosan composite used as an adsorbent for Cr(VI) in aqueous solutions. Int. *J. Biol. Macromol.* 2016, 87, 586-596.

[121] X.J. Hu, J.S. Wang, Y.G. Liu, X. Li, G.M. Zeng, Z.L. Bao, X.X. Zeng, A.W. Chen, F. Long, Adsorption of chromium (VI) by ethylenediamine-modified cross-linked magnetic chitosan resin: isotherms, kinetics and thermodynamics. *J. Hazard. Mater.* 2011, 185 (1), 306-314.

Acknowledgement

In the past three years and half, I have been studied in Kano Lab at the Graduate School of Science and Technology, Niigata University, Japan. Allow me to express my appreciations and thanks on my graduations.

Firstly, I would like to express my deepest gratitude to Associated Professor Naoki Kano for his sincerely guidance, valuable advice and encouragement, and I am very thanks to technical staff Mr. Naoto Miyamoto for his help for me throughout my doctoral course. I would like to thank Professor emeritus Hiroshi Imaizumi, Professor Tatsuya Kodama, Associated Professor Kenji Toda, Professor Hee-Joon Kim and Professor Takeshi Yamauchi for their advices and suggestions of this thesis.

Secondly, I also want to give my appreciations to peoples who give me many instructions, helping and encourage for my experiments. They are Dr. Kenji Mishima of Tsukuba University for his theoretical calculation, Mr. Haruo Morohashi of the Industrial Research Institute of Niigata Prefecture for the measurement of XPS, Ohizumi, M. of the Office for Environment and Safety, and Dr. Teraguchi, M., Mr. Nomoto, T., Prof. Tanaka, T and Hatamachi,T. of the Facility of Engineering in Niigata University for permitting the use of ICP-MS, FT-IR, SEM-EDS and Surface Area Analyzer for giving helpful advice in measurement, and my co-members my Chinese friends in our lab.

Finally, the best thanks to my parents and friends in China for their support of my studying abroad.